Dear Editor Gerd A. Folberth,

Please see attached our responses to the interactive comments for our papers entitled "A global scale mechanistic model of the photosynthetic capacity (LUNA V1.0)". We have carefully revised our manuscript based on the comments from the reviewers and editors. Please see in this file our specific responses and the revised manuscript with tracking changes. We hope that our manuscript is acceptable for publication in the GMD journal.

Yours
Chonggang

Chonggang Xu, Staff Scientist

Earth and Environmental Science Division

Los Alamos National Laboratory, NM, 87544

Web: https://sites.google.com/site/lanlveg

Email: cxu@lanl.gov

Phone: 505-665-9773

Responses to SC C1681

General comment to Executive editor: We greatly appreciate your time in checking of our paper to follow GMD journal requirements. The original comments of the reviewer are highlighted in red and our responses are in black. When text is copied directly from the revised paper the words are italicized.

Comment: Please note that for your paper, the following requirements have not been met in the Discussions paper:

"– The paper must be accompanied by the code, or means of accessing the code, for the purpose of peer-review. If the code is normally distributed in a way which could compromise the anonymity of the referees, then the code must be made available to the editor. The referee/editor is not required to review the code in any way, but they may do so if they so wish."

"– All papers must include a section at the end of the paper entitled "Code availability". In this section, instructions for obtaining the code (e.g. from a supplement, or from a website) should be included; alternatively, contact information should be given where the code can be obtained on request, or the reasons why the code is not available should be clearly stated."

"– All papers must include a model name and version number (or other unique identifier) in the title. " Please name LUNA v1.0 in the title and add a code availability section at the end (before the appendices) of the article upon your revised submission to GMD.

RESPONSE: We have now moved the "code availability" section before the "Appendix A" section. LUNA v1.0 is now incorporated in the title. The code availability section is modified in the revised manuscript as follows:

Code availability

This LUNA model has been implemented into CLM5.0 which will be openly available after its release in early 2016. Meanwhile, we have codes available in the form of MATLAB, FORTRAN and C#. They can be obtained upon request by sending an email to cxu@lanl.gov.

Responses to RC C1892

General comment to the reviewer: We greatly appreciate the constructive and thorough comments of this reviewer. We believe that these comments have led to improvements of our manuscript. We first repeat the comments of this reviewer before we detail our responses. The original comments of the reviewer are highlighted in red and our responses are in black. When text is copied directly from the revised paper the words are italicized.

Comment 1: The study uses two temperature functions to represent uncertainty of the temperature response of these parameters. TRF1 includes thermal acclimation of photosynthesis while TRF2 does not. There is a potential problem with using TRF2 as currently parameterized, as the optimum temperatures for Vcmax and Jmax do not vary in space on these simulations but we know they do in reality, therefore the assumption is that all C3 plants in the world are represented with the same temperature optimum for Vcmax and Jmax. How representative and valid are these values for cold adapted plants? Possibly, this has implications for some of the conclusions of the paper when taking
the difference between simulations with and without acclimation under both future and present day conditions. You could still have a simulation without thermal acclimation of photosynthesis, that accounts for special variability of Topt of Vcmax and Jmax (Kattge and Knorr, 2007, show the data, Medlyn et al 2002 as well). I think the authors ought to check /demonstrate whether this assumption (having a constant temperature optimum of Vcmax and Jmax on their non-acclimated temperature function) for has implications for their main conclusions.

RESPONSE: We appreciate this comment of the reviewer. He/she is correct in pointing out that TRF2 may not capture adequately "reality" by not accounting for thermal acclimation. That is one of the reasons why our model includes TRF1, which did account for thermal acclimations. In this work, we incorporated TRF2 because some Earth System Models do still not account for temperature acclimation. Hence, in our paper we list the corresponding values of the parameters of LUNA model for such type of Earth system models.

Furthermore, we feel that the comparison of TRF1 and TRF2 will help us analyze and quantify the impact of non-acclimation on our modeling results. Our results demonstrate that the two functions (TRF1 and TRF2) give similar results in almost all cases. Consequently, the main conclusion of our paper still holds, yet, some differences are observed in the values of $V_{c,max25}$ and the photosynthetic rate response to temperature. To better demonstrate how TRF2 impacts our results, we have modified the discussion section of our manuscript as follows (bold sentences highlight specifically the deficiency of TRF2).

Section 4.2 paragraph 1:

"*Our model predicts that higher temperatures generally lead to lower values of $V_{c,max25}$ and J_{max25} (Fig. 3a, c). As temperature increases, the nitrogen use efficiencies of $V_{c,max}$ and J_{max} also increase and thus plants need a lower amount of nitrogen allocated for carboxylation and electron transport. This is true for all the sites except for $V_{c,max25}$ in the hotter regions when*

TRF2 was used (Fig. S9a). The reason is because LUNA model will use a higher increase in night-time temperature (e.g., 22 to 30^{o}C) than daytime temperature (e.g., from 31 to 33^{o}C) , because the daytime temperature is constrained by the maximum temperature for optimization in TRF2 (i.e., 33^{o}C). To maximize the net photosynthetic carbon gain, the model predicts a higher proportion of nitrogen allocated to carboxylation to compensate for a higher nighttime respiration rate. Therefore, the LUNA model predicts a higher value of $V_{c,max25}$. ***Yet, this may result from the deficiency of TRF2 by not considering thermal acclimation under future global warming (Lombardozzi et al., 2015)."***

.

Section 4.2 paragraph 2:

" *If we do not account for the potential acclimation of $V_{c,max25}$ and $V_{c,max25}$ under future climate conditions as predicted by the LUNA model, our analysis indicates that ESM predictions of future global photosynthesis at the uppermost leaf layer will likely be overestimated by as much as 10-16% if $V_{c,max25}$ and J_{max25} are held fixed (Fig. 7).* ***The higher overestimation for TRF2 (16.3%) than TRF1 (10.1%) could result from the fact that TFR2 does not account for future thermal acclimation and thus the LUNA model predicts a large nitrogen allocation acclimation for future climate change.*** *In both cases, our results suggest that, to reliably predict global plant responses to future climate change, ESMs should incorporate models that use environmental control on $V_{c,max25}$ and J_{max25}. It has been recently suggested that nitrogen-related factors are not well represented in ESMs (Houlton et al., 2015; Wieder et al., 2015). Our nitrogen partitioning scheme would help alleviate biases into the predictions of future photosynthetic rates, and also climate processes that are dependent on these predictions (Bonan et al., 2011; Knorr and Kattge, 2005; Rogers, 2014).* "

Comment 2: There are other studies trying to do the same as this paper is doing, but based on empirical relationships (Verheijen et al 2013, Biogeosciences), between environmental drivers and Vcmax and Jmax at 25C, deriving relationships for each pft. The authors should acknowledge this type of work, which has also been used to extrapolate under future conditions (Verheijen et al 2015, GCB).

RESPONSE: We appreciate this comment of the reviewer. We have revised the paper to read on as follows:

"*…There are many different ways to incorporate environmental controls on $V_{c,max25}$ and J_{max25}. One simple approach is to use empirical statistical models between environmental variables and $V_{c,max25}$ and J_{max25} (e.g. Ali et al., 2015; Verheijen et al., 2013), which has been shown to improve the model simulations (Verheijen et al., 2015). One key limitation of such models is that they may have risk of inaccurate extrapolation under novel future climate conditions. The optimization*

model such as LUNA could be more reliable in their predictions under novel future climate conditions as they account for the key assumptions that could be robust under different environmental conditions. "

Comment 3: Missed paper on your references, Maire et al 2015, Global Ecol. Biogeog. See comments on soil ph, worth to include this on your limitations. The discussion on model limitations could also include the fact that there is inherent intraspecific variation of photosynthetic capacity (See Moran et al. 2015, GCB).

RESPONSE: We have now incorporated the above references in the model limitation section of our revised paper. For instance, the first two paragraphs in section 4.1 as follows (bolded sentences):

"…These results suggest that our model is able to capture many of the key components of the drivers for $V_{c,max25}$ and J_{max25} across the globe both in space as well as in time. The remaining portion of uncertainty that cannot be explained by our *LUNA* model could be related to variability within the 125 species considered in this study. ***There are inherent intraspecific variations in leaf traits (Valladares et al., 2000) and in photosynthetic capacity (Moran et al., 2015).*** Data availability limited the number of species that can be considered and favored a universal *LUNA* model as separate species normally did not cover a sufficiently large range of environmental conditions. Yet, we should be able to fit our model to specific PFTs when additional data become available with a large enough coverage of environmental conditions. We expect that such a model would be able to describe and capture adequately a larger portion of the variability observed in $V_{c,max25}$ and $J_{max25.}$

Unexplored nutrient limitations and other plant physiological properties could also play a factor in the limitation of our model. For example, the nitrogen use efficiency of tropical plants (typically modest to low nitrogen) can be diminished by low phosphorus (Cernusak et al., 2010; Reich and Oleksyn, 2004), suggesting that our model could be improved by considering multiple nutrient limitations (Goll et al., 2012; Walker et al., 2014; Wang et al., 2010). Our treatment of photosynthetic capacity could also be improved by incorporating species-specific mesophyll and stomatal conductance (Medlyn et al., 2011), by analyzing leaf properties such as leaf life span (Wright et al., 2004), or ***by considering soil nutrient, soil water availability, and soil pH (Maire et al., 2015)***. "

Comment 4: There are a lot more papers out using optimization now, perhaps you should cite them too.

RESPONSE: We agree with the reviewer and have modified the text in the revised paper to discuss this at end of section 4.2 as follows:

"…*By far, the optimality approaches have been used to predict many different plant structures and functions under different environmental conditions such as carbon allocations (Franklin et al., 2012), leaf C:N (Thomas and Williams, 2014), root distribution (McMurtrie et al., 2012), and stomata conductance (Cowan and Farquhar, 1977). For the photosynthetic capacity optimization, Haxeltine and Prentice (1996) has used an optimization approach to predict* $V_{c,max25}$ *based on the trade-off between photosynthesis and respiration, which has been incorporated into land surface models including LPJ-GUESS (Smith et al., 2001) and LPJmL (Sitch et al., 2003). Both LUNA model and the model of Haxeltine and Prentice (1996)*

considered the $V_{c,max25}$ component and respiration; however, LUNA model is currently only designed for the leaf level while model of Haxeltine and Prentice (1996) is applicable for both the leaf and canopy level. The key improvements of LUNA model include the explicit considerations of other important processes such as light capture and electron transport and 2) the evaluations against global datasets under different environmental conditions".

Comment 5: Page 6221, line 15, replace 'need' with 'needs'

RESPONSE: We have replaced "need" with "needs" now.

Comment 6: Page 6222, lines 21-22 replace 'Optimal approaches are an important tool of land surface models', with Optimal approaches are an important tool for land surface models. Page 6224, lines 7-8 & 14 no need to repeat references on line 8 when already given in line 7 Page 6224, define MCMC.

RESPONSE: On page 6222, lines 21-22, we have replaced "Optimal approaches are an important tool of land surface models" with "Optimality approaches are important tools for land surface models". We have eliminated the references in lines 8 and 14 on page 6224. Also, we now spell out MCMC as Markov Chain Monte Carlo in the revised paper.

Comment 7: Although you do not specify pfts on your model, it would be good to give an idea to the reader (most probably a modeler) of the geographical distribution of your data set (used to calibrate your model) in terms of plant functional types.

RESPONSE: We have now incorporated a map of data distribution in the supplementary file and it is now referenced in the data section as follows:

"*….The data include evergreen and deciduous species from arctic, boreal, temperate and tropical areas measured different times of the season and different canopy locations (Fig. S2).*"

See the figure below:

Fig . S2 *The spatial distribution map of data used for parameter estimation in LUNA model*

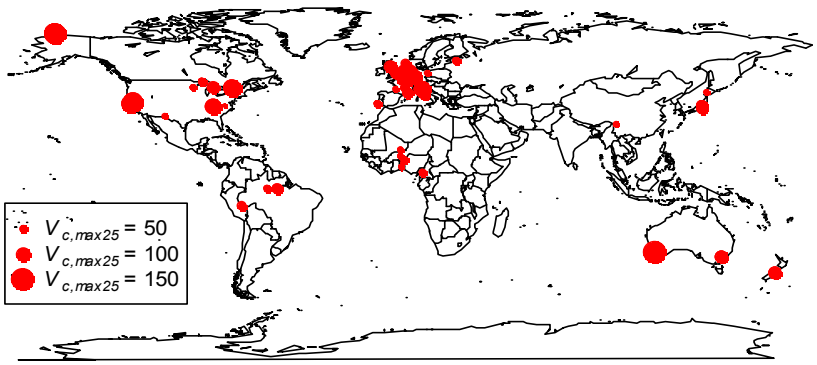

Comment 8: Parameter estimation and evaluation is done with same data set. Please comment on implications of this. I wonder if you could fit the model with a portion of the data, then use your LUNA to predict Vcmax and Jmax and then evaluate the goodness of the model.

Response: We agree with the reviewer that it is a good idea to use a subset of data for parameter estimation and another subset of data for evaluation of the goodness of fit of the model. In this study, our focus was to develop a mechanistic model of photosynthetic capacity for the globe and so we did not use subsets of data for parameter estimation and model evaluation in view that we have a limited number of data points across the globe. It would be challenge to randomly select a large subset of data for model evaluation. For the case of small subset, we expect that it should not be much different from the model fitting we currently have as it will be mainly based on a large portion of the data. In a new project, we are collecting independent data from the tropics and it would be great independent test against LUNA model. We hope to publish the new paper soon.

Comment 9: Section 2.6 is model sensitivity analysis. Then on p 6227 another sensitivity is mentioned, is this the same?, why to have it twice, confusing and repetitive

RESPONSE: Thank you very much for pointing this out. The section 2.6 sensitivity analysis is for the fitted model using fitted parameter and mean environmental conditions from the data. It is only for one specific environmental condition under current climate condition. The sensitivity analysis on p6227 is for the whole globe to assess which variable change in the future are responsible for the change in $V_{c,max}$ and J_{max} and the environmental condition change could be different for different locations across the globe. To clarify this, we have improved the statement on p6227 as follows:

"*….In order to identify the importance of changes in different climate variables (temperature, CO_2, radiation and relative humidity) to modeled changes in $V_{c,max25}$ and J_{max25} in the future, we conducted a third sensitivity analysis to investigate the impact of changes in climate variables on model results. In contrast to the previous two sensitivity analyses that based on the mean current climate conditions, the purpose of the third sensitivity analysis was to explore the global pattern in sensitivity of $V_{c,max25}$ and J_{max25} to changes in climate variables across different biomes of the globe in the future*".

Comment 10: Fig 4 & 5, very poor color scale as it does not show much of the variation on key ecosystems.

RESPONSE: We have now improved the color scale of Figures 4 as follows:

Figure 4 Summer season photosynthetic capacity for the top leaf layer in the canopy ($V_{c,max25}$; μmol CO_2 m^{-2} s^{-1} (a), J_{max25}; μmol electron m^{-2} s^{-1} (c)) under historical climatic conditions and the difference in either $V_{c,max25}$ (b) or J_{max25} (d) due to changed climatic conditions. Difference in the photosynthetic capacity was calculated as that under future climate minus that under historical climate. Ten-year monthly averages of climatic conditions for the past (1995 – 2004) and the future (2090-2099) were used to drive the model. The model was run by using TRF1, which was a temperature response function that considered the potential for acclimation to growth temperature.

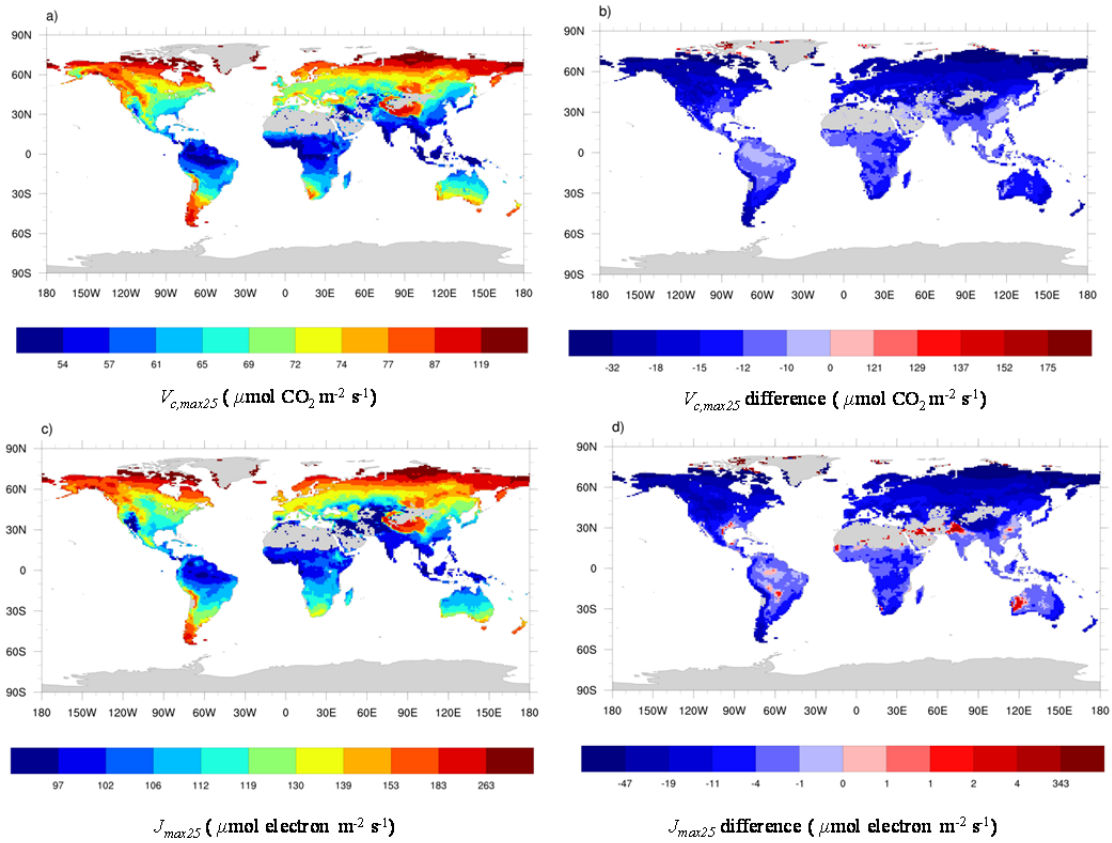

Following Fig. 4, we also changed the color legends in Fig S6 (or Fig. S8 in revised manuscript) correspondingly.

For Fig. 5, because we want to have on common legend for all panels in order to compare the sensitivities of different climate variables, it would be challenging to make each panel show the range of major ecosystems if their changes are small. Therefore, we keep it as it is.

Comment 10: Fig 5, is this the + or the minus 15% sensitivity?, not clear in the Fig caption

RESPONSE: No, it is not based on 15% change. The sensitivity analysis is conducted by changing the environmental variable using 10-year monthly averages of climatic conditions for the past (1995-2004) versus the future (2090-2099). For clarification, we have modified the captions of Fig. 5 and 6 as follows:

"*…The sensitivity analysis is conducted by changing the value of individual environmental variable using 10-year monthly averages of climatic conditions for the past (1995-2004) versus the future (2090-2099) for each individual grid across the globe*."

Comment 11: P 6229., Lines 25-26 replace '.It also well captured ..' with It also captured well '

RESPONSE: We have changed the statement to "it also captured well"

Comment 12: P 6232, L10, you mean high growing season temperatures?, add word 'season'

RESPONSE: We have improved to statement to reflect "high growing season temperatures"

References

Ali, A. A., Xu, C., Rogers, A., McDowell, N. G., Medlyn, B. E., Fisher, R. A., Wullschleger, S. D., Reich, P. B., Vrugt, J. A., Bauerle, W. L., Santiago, L. S., and Wilson, C. J.: Global scale environmental control of plant photosynthetic capacity, Ecological Applications, doi: 10.1890/14-2111.1, 2015. 2015.

Bonan, G. B., Lawrence, P. J., Oleson, K. W., Levis, S., Jung, M., Reichstein, M., Lawrence, D. M., and Swenson, S. C.: Improving canopy processes in the community land model version 4 (CLM4) using global flux fields empirically inferred from FLUXNET data, Journal of Geophysical Research, 116, 1-22, 2011.

Cernusak, L. A., Winter, K., and Turner, B. L.: Leaf nitrogen to phosphorus ratios of tropical trees: experimental assessment of physiological and environmental controls, New Phytologist, 185, 770-779, 2010.

Cowan, I. and Farquhar, G.: Stomatal function in relation to leaf metabolism and environment, 1977, 471-505.

Franklin, O., Johansson, J., Dewar, R. C., Dieckmann, U., McMurtrie, R. E., Brännström, Å., and Dybzinski, R.: Modeling carbon allocation in trees: a search for principles, Tree Physiology, 32, 648-666, 2012.

Goll, D. S., Brovkin, V., Parida, B. R., Reick, C. H., Kattge, J., Reich, P. B., van Bodegom, P. M., and Niinemets, U.: Nutrient limitation reduces land carbon uptake in simulations with a model of combined carbon, nitrogen and phosphorus cycling, Biogeosciences, 9, 3547-3569, 2012.

Haxeltine, A. and Prentice, I. C.: A general model for the light-use efficiency of primary production, Functional Eocolgy, 10, 551-561, 1996.

Houlton, B. Z., Marklein, A. R., and Bai, E.: Representation of nitrogen in climate change forecasts, Nature Clim. Change, 5, 398-401, 2015.

Knorr, W. and Kattge, J.: Inversion of terrestrial ecosystem model parameter values against eddy covariance measurements by Monte Carlo sampling, Global Change Biology, 11, 1333-1351, 2005.

Lombardozzi, D. L., Bonan, G. B., Smith, N. G., Dukes, J. S., and Fisher, R. A.: Temperature acclimation of photosynthesis and respiration: A key uncertainty in the carbon cycle-climate feedback, Geophysical Research Letters, 42, 8624-8631, 2015.

Maire, V., Wright, I. J., Prentice, I. C., Batjes, N. H., Bhaskar, R., van Bodegom, P. M., Cornwell, W. K., Ellsworth, D., Niinemets, Ü., Ordonez, A., Reich, P. B., and Santiago, L. S.: Global effects of soil and climate on leaf photosynthetic traits and rates, Global Ecology and Biogeography, 24, 706-717, 2015.

McMurtrie, R. E., Iversen, C. M., Dewar, R. C., Medlyn, B. E., Näsholm, T., Pepper, D. A., and Norby, R. J.: Plant root distributions and nitrogen uptake predicted by a hypothesis of optimal root foraging, Ecology and Evolution, 2, 1235-1250, 2012.

Medlyn, B. E., Duursma, R. A., Eamus, D., Ellsworth, D. A., Prentice, I. C., Barton, C. V. M., Crous, K. Y., De Angelis, P., Freeman, M., and Wingate, L.: Reconciling the optimal and empirical approaches to modelling stomatal conductance, Global Change Biology, 10, 1365-2486, 2011.

Moran, E. V., Hartig, F., and Bell, D. M.: Intraspecific trait variation across scales: implications for understanding global change responses, Global Change Biology, doi: 10.1111/gcb.13000, 2015. n/a-n/a, 2015.

Reich, P. B. and Oleksyn, J.: Global patterns of plant leaf N and P in relation to temperature and latitude, PNAS, 101, 11001-11006, 2004.

Rogers, A.: The use and misuse of $V_{c,max}$ in earth system models, Photosynthesis Research, 119, 1-15, 2014.

Sitch, S., Smith, B., Prentice, I. C., Arneth, A., Bondeau, A., Cramer, W., Kaplan, J. O., Levis, S., Lucht, W., Sykes, M. T., Thonicke, K., and Venevsky, S.: Evaluation of ecosystem dynamics, plant geography and terrestrail carbon cycling in the LPJ dynamic global vegetation model, Global Change Biology, 9, 161-185, 2003.
Smith, B., Prentice, I. C., and Sykes, M. T.: Representation of vegetation dynamics in the modelling of terrestrial ecosystems: comparing two contrasting approaches within European climate space, Global Ecology and Biogeography, 10, 621-637, 2001.
Thomas, R. Q. and Williams, M.: A model using marginal efficiency of investment to analyze carbon and nitrogen interactions in terrestrial ecosystems (ACONITE Version 1), Geosci. Model Dev., 7, 2015-2037, 2014.
Valladares, F., Wright, S. J., Lasso, E., Kitajima, K., and Pearcy, R. W.: PLASTIC PHENOTYPIC RESPONSE TO LIGHT OF 16 CONGENERIC SHRUBS FROM A PANAMANIAN RAINFOREST, Ecology, 81, 1925-1936, 2000.
Verheijen, L. M., Aerts, R., Brovkin, V., Cavender-Bares, J., Cornelissen, J. H. C., Kattge, J., and van Bodegom, P. M.: Inclusion of ecologically based trait variation in plant functional types reduces the projected land carbon sink in an earth system model, Global Change Biology, 21, 3074-3086, 2015.
Verheijen, L. M., Brovkin, V., Aerts, R., Bönisch, G., Cornelissen, J. H. C., Kattge, J., Reich, P. B., Wright, I. J., and van Bodegom, P. M.: Impacts of trait variation through observed trait–climate relationships on performance of an Earth system model: a conceptual analysis, Biogeosciences, 10, 5497-5515, 2013.
Walker, A. P., Beckerman, A. P., Gu, L., Kattge, J., Cernusak, L. A., Domingues, T. F., Scales, J. C., Wohlfahrt, G., Wullschleger, S. D., and Woodward, F. I.: The relationship of leaf photosynthetic traits – Vcmax and Jmax – to leaf nitrogen, leaf phosphorus, and specific leaf area: a meta-analysis and modeling study, Ecology and Evolution, 4, 3218-3235, 2014.
Wang, Y. P., Law, R. M., and Pak, B.: A global model of carbon, nitrogen and phosphorus cycles for the terrestrial biosphere, Biogeosciences, 7, 2261-2282, 2010.
Wieder, W. R., Cleveland, C. C., Lawrence, D. M., and Bonan, G. B.: Effects of model structural uncertainty on carbon cycle projections: biological nitrogen fixation as a case study Environmental Research Letters, 10, 044016, 2015.
Wright, I. J., Reich, P. B., Westoby, M., Ackerly, D. D., Baruch, Z., Bongers, F., Cavender-Bares, J., Chapin, T., Cornelissen, J. H. C., Diemer, M., Flexas, J., Garnier, E., Groom, P. K., Gulias, J., Hikosaka, K., Lamont, B. B., Lee, T. D., Lee, W., Lusk, C. H., Midgley, J. J., Navas, M.-L., Niinemets, Ü., Olesksyn, J., Osada, N., Poorter, H., Poot, P., Prior, L., Pyankov, V. I., Roumet, C., Thomas, S. C., Tjoelker, M. G., Veneklaas, E. J., and Villar, R.: The worldwide leaf economics spectrum, Nature, 428, 821-827, 2004.

Responses to SC2218

General comment to the reviewer: We thank the reviewer for his/her constructive comments and we address the various concerns below. The original comments of the reviewer are highlighted in red and our responses are in black. When text is copied directly from the revised paper the words are italicized.

Comment 1: Ali et al. set up an optimality criterion: available leaf N is allocated in such a way as to "maximize the photosynthetic carbon gain". As a result of applying this criterion they can account for key features of observed patterns today. But then when applying the optimization principle to a climate-change scenario they find a substantial reduction in future global photosynthesis, compared to a reference simulation in which photosynthetic capacities were held constant. This does not appear to me to make any sense. How can optimizing carbon gain lead to reduced carbon gain? I have tried to trace how the result arises but I am still not clear, and therefore I would like the authors to clarify the result, and especially to comment on its plausibility.
Based on the text as it is, my understanding is that it may result from the restriction in TRF2 (applied in warmer climates) that optimization of photosynthetic capacity does not continue to temperatures above 33 C (although leaf temperatures higher than this are commonly encountered in tropical forest canopies!) whereas respiration, much of which happens at night, continues to increase with temperature. If this is the explanation, then the result is an artefact of the assumptions of the study: i.e. that photosynthetic acclimation stops at 33 C, while respiration will continue to increase with temperature – even if the additional respiration has no useful function for the plant.

RESPONSE: We thank the reviewer for highlighting his concern.

Thank you very much for identifying this important confusion point in your reading of our paper. It is important to point out that the "optimization" in LUNA model is to maximize the net photosynthetic carbon gain (defined as gross photosynthesis minus the maintenance respiration for photosynthetic enzyme) given the plant's strategy of leaf nitrogen use built into LUNA model. Namely, it is a conditional optimization. Thus, it is possible that values of $V_{c,max\ 25}$ and J_{max25} other than the "optimal" values predicted by LUNA model could have a higher net photosynthetic rate, if the plant does not follow the prescribed plant nitrogen use strategy built into the LUNA model. For a better understanding of the conditional optimization, we incorporate the following section under "model description section" in the revised paper.

"*… It is important to point out that the optimization in LUNA model is a conditional optimization given the plant's nitrogen use strategies built into the model. Thus, it is possible that "optimal" values of* $V_{c,max\ 25}$ *and* J_{max25} *predicted by the LUNA model for future climate conditions could have a lower net photosynthetic carbon gain compared to fixed values of* $V_{c,max\ 25}$ *and* J_{max25}*, where the plant does not follow the nitrogen use strategies built into the LUNA model. An example is shown in Fig. S1 where the "optimal" net photosynthetic carbon gain using the nitrogen allocation predicted by LUNA model for the elevated temperature is lower than that using fixed nitrogen allocation predicted for the ambient temperature.* "

The new Figure S1 is as follows:

Figure S1 *Illustration of conditional optimization in the LUNA model. In the model, the nitrogen use patterns vary under different environmental conditions. For example, the net photosynthetic carbon gain vs nitrogen allocation to light capture under ambient temperature (mean daytime temperature at 14.75 ^{o}C and mean night time temperature at 11. 45 ^{o}C; blue line) is different from that under the elevated temperature (+5 ^{o}C; red line). Therefore, the "optimal" net photosynthetic carbon gain under elevated temperature (red point) could be lower than the net photosynthetic carbon gain (green point) under elevated temperature using optimal parameters (the nitrogen allocations) under ambient temperature.*

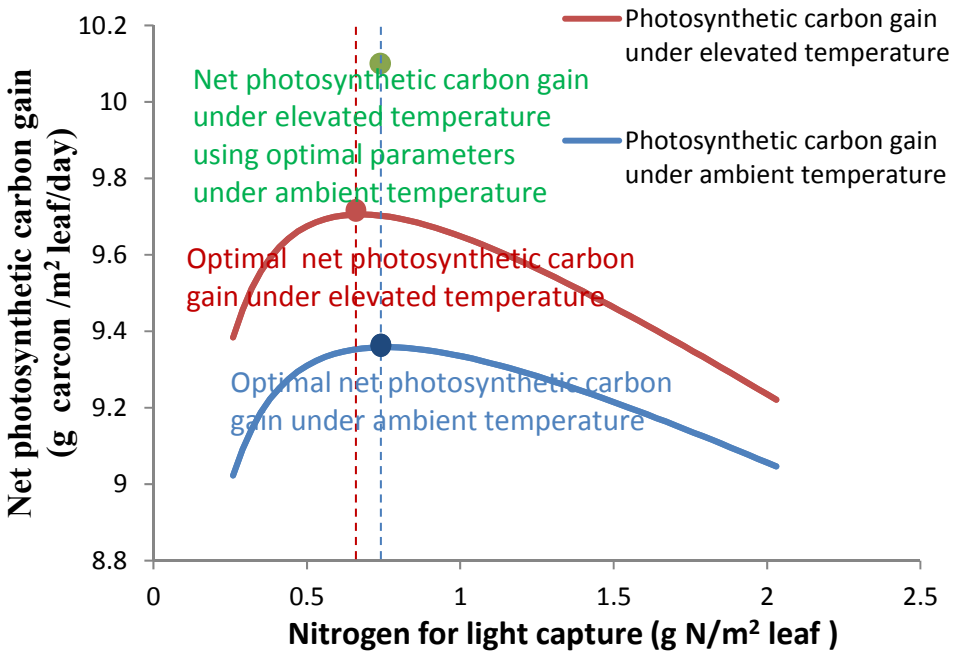

Responses to RC2826

General comment to the reviewer: Thank you very much for carefully reading through the manuscript and providing the constructive comments. The original comments of the reviewer are highlighted in red and our responses are in black. When text is copied directly from the revised paper the words are italicized.

Comment 1: I'm still confused about if the model needs total leaf nitrogen per unit leaf area (LNCa) and leaf mass per area (LMA) as input, after reading through the paper a couple of times and carefully tracing all the equations in appendixes. Thus, I have to discuss it in two cases: 1) the model needs the LNCa and LMA as input and 2) the model does NOT need the LNCa and LMA as input

CASE I: the model needs the LNCa and LMA as input In Appendix A, the authors described total leaf nitrogen, structural N (as a function of LMA), and N storage. It seems the model needs the total leaf nitrogen per unit leaf area (LNCa) and leaf mass per area (LMA) as input. What the model does is to properly allocate the LNCa to different functional and storage components to get leaf's photosynthesis carbon gain maximized. Since leaf nitrogen (i.e., LNCa in this paper) and LMA are good predictors of photosynthesis capacity, it's not surprising to see this model can explain more than 50% variances of Vcmax25 and Jmax25 (57% and 66%, respectively). I'd like to see the improvement of the predictions of Vcmax25 and Jmax25 from LUNA model comparing to those directly derived from LNCa and LMA. And, the authors should make it clear how they obtained the data of leaf Nitrogen and LMA at global scale.

RESPONSE: CASE I is applicable to the LUNA model. For clarification, we have added the following component into the model description section:

"*The model uses area-based leaf nitrogen content and different environmental conditions (temperature, CO_2, radiation, relative humidity and day length) as model inputs and predicts $V_{c,max\ 25}$ and J_{max25} based on the optimal amount of nitrogen allocated to different processes*."

Following the suggestions of comparing LUNA model with a statistical model only with LNCa and leaf mass per unit area (LMA), we have added the improvement of the predictions of $V_{c,max25}$ and J_{max25} from LUNA model comparing to those directly derived from LNCa and LMA in the first paragraph of discussion on "model limitation".

"*….The assumption that nitrogen is allocated according to optimality principles explained a large part of variability in $V_{c,max25}$ (~ 55%) and in J_{max25} (~ 65%) at the global scale, regardless of the temperature response functions used. It also captured well the seasonal cycles and the PFT-specific values of $V_{c,max25}$ and J_{max25} (Fig. S3-5).* ***It has a much improved fitting to the data in comparison to a multi-linear regression model using LNC_a and LMA as predictors, which only explained ~22% of the variance in observed $V_{c,max25}$ (Fig. S12 a, d) and ~13% of the variance in observed J_{max25} (Fig. S12b, d) for both temperature response functions.*** *These results suggest our model is able to capture many of the key components of the drivers of $V_{c,max25}$ and J_{max25} across the globe both in space as well as in time*."

See the new figure is shown below:

Figure S12 *Percentage of variations (r^2, ME; model efficiency) in observed $V_{c,max25}$ (μmol CO_2 m^{-2} s^{-1}) explained by modeled $V_{c,max25}$ (a; TRF1, c; TRF2) and in observed J_{max25} (μmol electron m^{-2} s^{-1}) explained by modeled J_{max25} (b; TRF1, d; TRF2) by using a multi-linear regression over leaf nitrogen content (g N/m^2 leaf) and the leaf mass per unit area (g dry mass /m^2 leaf). The nitrogen allocation model was run with the environmental variables, leaf mass per leaf area, and the leaf nitrogen contents by using TRF1. TRF1 was a temperature response function that considered the potential for acclimation to growth temperature. The r^2 is derived by a linear regression between observed and modeled values. The dashed line is the 1:1 line.*

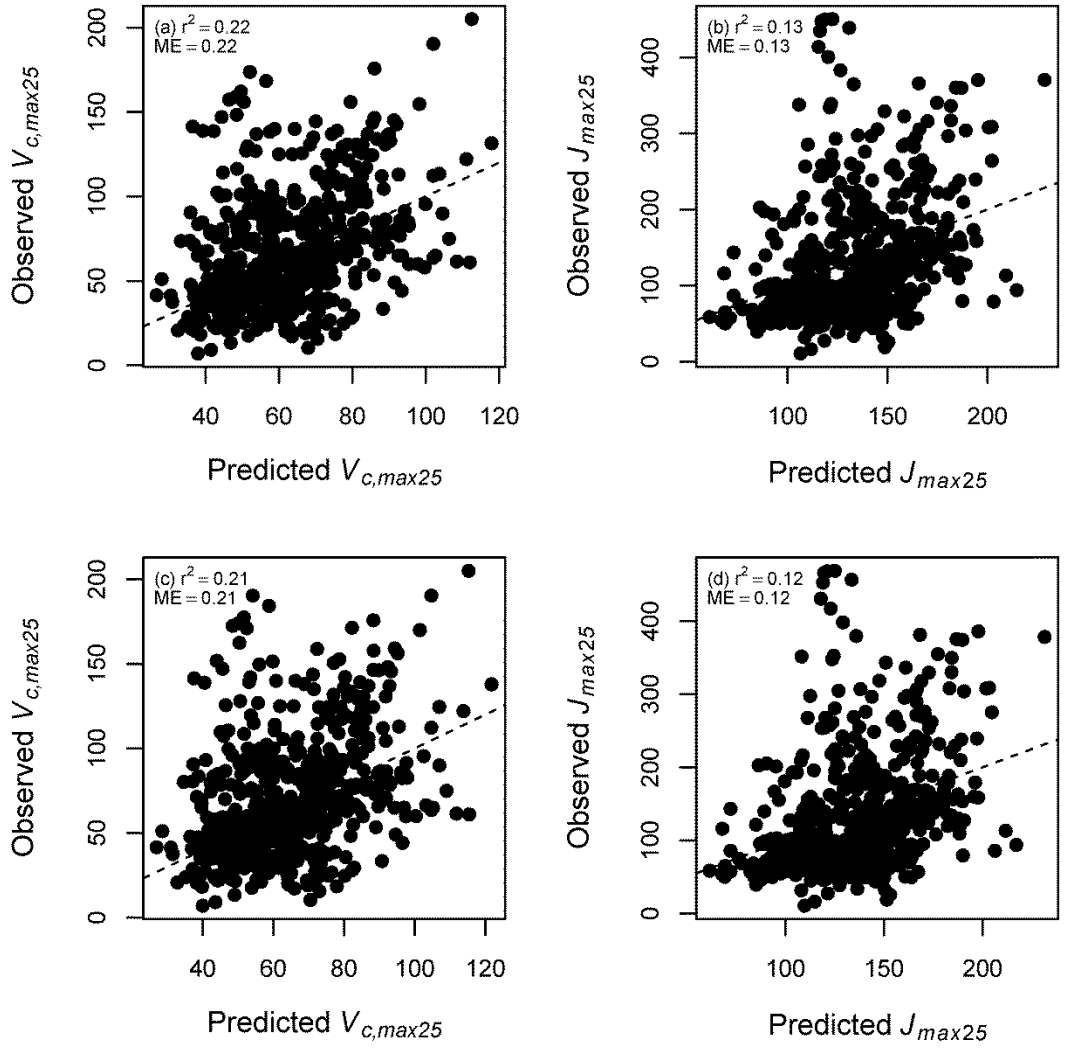

We have added the following section in the data section of revised paper for clarification on how we collected the data:

"*…Specifically, we conducted a literature search on Google Scholar to locate publications that included words "$V_{c,max}$" or "J_{max}" and also contained "leaf nitrogen content" , "maximum carboxylation rate" , "maximum electron transport rate" , "leaf mass per area", or "specific leaf area". Individual values of $V_{c,max}$, J_{max}, area-based leaf nitrogen content (LNC_a, g N/m^2 leaf) and leaf mass per unit leaf area (LMA, g dry mass/ m^2 leaf) were then obtained by digitizing data from the literature.*"

Comment 2: CASE II: the model doesn't need the LNCa and LMA as input In the main text, they said "the key drivers (temperature, radiation, humidity, CO2, and day length) (Lines 26_27, Page 6220)". It seems the model doesn't need the LNCa and LMA as input. In this case, the Nitrogen supply is assumed to be unlimited or the leaf is infinitely small. The variables of total leaf nitrogen (LNCa), structural N, functional
nitrogen (FNCa), and Nitrogen storage (Nstore) are not solvable according to the equations of this model of LNCa is unknown. The Nitrogen for light capture (Nlc), electron transport (Net), carboxylation (Ncb), and respiration (Nresp) can be obtained numerically only when the respiration rate increases faster than photosynthesis with Nlc. Otherwise there will be no equilibrium point (i.e., N for photosynthesis and respiration will go to infinitely large) and the model is not solvable. Thus, this model must be very sensitive to respiration parameters.
If it's this case, the model is useful for predicting potential Vcmax and Jmax according to the climatic variables. But the assumptions must be clearly stated and justified. As I can see from the paper, the assumptions include: there is only one leaf for each land unit and the leaf is very small; N is unlimited; Ra and photosynthes are functions of N, but Ra increases faster than photosynthesis with N. The authors designed a set of parameters to constrain the relative abundances of Nlc, Net, Ncb, and Nresp. These parameters can be categorized into two classes: photosynthesis processes, and respiration processes. And they were fixed in this paper to make sure respiration increases faster than photosynthesis with leaf N. For a canopy, this pattern (i.e., respiration rate increases faster than photosynthesis with leaf N) is true because of the light gradient within the canopy. But I can't figure it out how it holds in a single leaf without other limitations. You can imagine that with each function apparatus, there is a set of Nlc, Net, Ncb, and Nresp and the carbon balance is positive (photosynthesis > respiration). If N is unlimited and no other limitations (e.g., structural limitations of a leaf), a leaf can have infinite such photosynthesis apparatuses and the carbon balance is still positive. Actually, whatever how many the apparatuses are, the ratio of respiration to photosynthesis is the same at given climatic conditions. I want the authors to explain it.

RESPONSE: CASE II does NOT apply to our model. That is, the LUNA model needs the LNCa and LMA as inputs.

MS with tracking of changes in red

A global scale mechanistic model of the photosynthetic capacity (LUNA V1.0)

ASHEHAD A. ALI[1,2], CHONGGANG XU[1*], ALISTAIR ROGERS[3], ROSIE A. FISHER[4], STAN D. WULLSCHLEGER[5], NATE G. MCDOWELL[1], ELIAS C. MASSOUD[2], JASPER A. VRUGT[2,6], JORDAN D. MUSS[1], JOSHUA B. FISHER[7], PETER B. REICH[8,9], CATHY J. WILSON[1]

1. Earth and Environmental Sciences Division, Los Alamos National Laboratory, Los Alamos, New Mexico, USA
2. Department of Civil and Environmental Engineering, University of California Irvine, Irvine, California, USA
3. Biological, Environmental and Climate Sciences Department, Brookhaven National Laboratory, Upton, New York, USA
4. Climate and Global Dynamics, National Center for Atmospheric Research, Boulder, Colorado, USA
5. Climate Change Science Institute, Environmental Sciences Division, Oak Ridge National Laboratory, Oak Ridge, Tennessee, USA
6. Department of Earth System Science, University of California Irvine, Irvine, California, USA
7. Jet Propulsion Laboratory, California Institute of Technology, Pasadena, California, USA
8. Department of Forest Resources, University of Minnesota, St. Paul, Minnesota, USA
9. Hawkesbury Institute for the Environment, University of Western Sydney, Penrith, New South Wales, Australia

[*]Corresponding author(s), Email: xuchongang@gmail.com (CX)

Abstract

Although plant photosynthetic capacity as determined by the maximum carboxylation rate (i.e., $V_{c,max25}$) and the maximum electron transport rate (i.e., J_{max25}) at a reference temperature (generally 25°C) is known to vary substantially in space and time in response to environmental conditions, it is typically parameterized in Earth system models (ESMs) with tabulated values associated to plant functional types. In this study, we developed a mechanistic model of leaf utilization of nitrogen for assimilation (LUNA V1.0) to predict the photosynthetic capacity at the global scale under different environmental conditions, based on the optimization of nitrogen allocated among light capture, electron transport, carboxylation, and respiration. The LUNA model was able to reasonably ~~well~~ capture the observed patterns of photosynthetic capacity ~~in view that~~as it explained approximately 55% of the variation in observed $V_{c,max25}$ and 65% of the variation in observed J_{max25} across the globe. Our model simulations under current and future climate conditions indicated that ~~$V_{c,max25}$ could be~~simulations of $V_{c,max25}$ based on this new optimization strategy were most affected in high-latitude regions under a warming climate and that ESMs using a fixed $V_{c,max25}$ or J_{max25} by plant functional types were likely to substantially overestimate future global photosynthesis.

Keywords: carbon cycle, climate variables, leaf nitrogen optimization and model-data synthesis

1. Introduction

Photosynthesis is one of the major components of the ecosystem carbon cycle ~~(Canadell et al., 2007; Sellers et al., 1997)~~(Canadell et al., 2007; Sellers et al., 1997) and is thus central to Earth system models (ESMs) (Block and Mauritsen, 2013; ~~Hurrell et al., 2013~~Hurrell et al., 2013). Most of the ESMs are based on photosynthesis models developed by Farquhar et al. ~~(1980)~~(1980), which are particularly sensitive to photosynthetic capacity. The maximum carboxylation rate scaled to 25°C [i.e., $V_{c,max25}$ (μmol CO_2 m^{-2} s^{-1})] and the maximum electron transport rate scaled to 25°C [i.e., J_{max25} (μmol electron m^{-2} s^{-1})] have been generally accepted as the measure of photosynthetic capacity. $V_{c,max25}$ and J_{max25} are the key biochemical parameters in the photosynthesis models as they control the carbon fixation process ~~(Farquhar et al., 1980)~~(Farquhar et al., 1980). There exist large variations in estimates of gross primary productivity in space and time across ESMs ~~(Schaefer et al., 2012)~~(Schaefer et al., 2012), which have been partly attributed to uncertainties in $V_{c,max25}$ (Bonan et al., 2011). Accurate estimations of $V_{c,max25}$ and J_{max25} are needed to simulate gross primary productivity because errors of $V_{c,max25}$ and J_{max25} may be exacerbated when upscaling from leaf to ecosystem level ~~(Hanson et al., 2004)~~(Hanson et al., 2004).

Our ability to make reliable predictions of $V_{c,max25}$ and J_{max25} at a global scale is limited. One of the reasons is that we do not have a complete understanding of the processes influencing $V_{c,max25}$ and J_{max25} ~~(Maire et al., 2012; Xu et al., 2012)~~(Maire et al., 2012; Xu et al., 2012) despite the fact that $V_{c,max25}$ has been measured and studied more extensively than many other photosynthetic parameters ~~(Kattge and Knorr, 2007; Leuning, 1997; Wullschleger, 1993)~~(Kattge and Knorr, 2007; Leuning, 1997; Wullschleger, 1993). Many empirical studies have shown that $V_{c,max25}$ and J_{max25} (or field-based surrogates) correlate with leaf nitrogen content ~~(Medlyn et al.,~~

1999; Prentice et al., 2014; Reich et al., 1998; Ryan, 1995; Walker et al., 2014)(Medlyn et al., 1999; Prentice et al., 2014; Reich et al., 1998; Ryan, 1995; Walker et al., 2014). Therefore, a constant relationship between the leaf nitrogen content and $V_{c,max25}$ or J_{max25} is commonly utilized by many ecosystem models (Bonan et al., 2003; Haxeltine and Prentice, 1996; Kattge et al., 2009); Haxeltine and Prentice, 1996; Kattge et al., 2009). The relationship between leaf nitrogen content, $V_{c,max25}$ and J_{max25} varies with different light, temperature, nitrogen availability and CO_2 conditions (Friend, 1991; Reich et al., 1995; Ripullone et al., 2003)(Friend, 1991; Reich et al., 1995; Ripullone et al., 2003), and therefore, the prescribed relationship of $V_{c,max25}$, J_{max25} and leaf nitrogen content might introduce significant biases into predictions of future photosynthetic rates, and also the downstream carbon cycle and climate processes that are dependent on these predictions (Bonan et al., 2011; Knorr and Kattge, 2005Knorr and Kattge, 2005; Rogers, 2014Rogers, 2014).

To better account for the relationships between photosynthetic capacities and their environmental determinants, we developed a mechanistic model of leaf utilization of nitrogen for assimilation (LUNA V1.0) at the global scale that accounts for the key drivers (temperature, radiation, humidity, CO_2 and day length) contributing to the variability in the relationship between leaf nitrogen, $V_{c,max25}$ and J_{max25}. Based on the theoretically optimal amount of leaf nitrogen allocated to different processes, the LUNA model predicts $V_{c,max25}$ and J_{max25} under different environmental conditions. We estimate the LUNA model parameters by fitting the model predictions to observations of $V_{c,max25}$ and J_{max25}. In order to assess the impacts of future climate change on photosynthesis, we used the calibrated *LUNA* model to estimate the summer season net photosynthetic rate using predicted V_{cmax25} and J_{max25} under historical and future

climate conditions. We conclude that ESMs using a fixed $V_{c,max25}$ or J_{max25} by plant functional types (PFTs) are likely to substantially overestimate future global photosynthesis.

2. Methodology

2.1. Overview

Our *LUNA* model (version 1.0) is based on the nitrogen allocation model developed by Xu et al. ~~(2012)~~(2012), which optimizes nitrogen allocated to light capture, electron transport, carboxylation, and respiration. Xu et al. ~~(2012)~~(2012) considered a series of assumptions on the model to generate optimized nitrogen distributions, these were (*i*) that storage nitrogen is allocated to meet requirements to support new tissue production; (*ii*) respiratory nitrogen is equal to the demand implied by the sum of maintenance respiration and growth respiration; (*iii*) light capture, electron transport and carboxylation are co-limiting to maximize photosynthesis. Xu et al.'s model ~~need~~needs to be calibrated, and has thus far been tested for three ~~test~~ sites. Here, we expand on the work of Xu et al. ~~(2012)~~(2012) to allow global predictions of nitrogen allocation, by fitting the model parameters to an expanded photosynthetic capacity data set. To make global predictions feasible, we also made important refinements to ~~Xu et al.'s~~the model by considering the impacts of both day length and humidity, and the variations in the balance between light-limited electron transport rate and the Rubisco-limited carboxylation rate in accordance with recent theory. We used an efficient Markov Chain Monte Carlo simulation approach, the Differential Evolution Adaptive Metropolis Snooker Updater (DREAM-ZS) algorithm ~~(Laloy and Vrugt, 2012)~~(Laloy and Vrugt, 2012), to fit the nitrogen allocation model to a large dataset of observed $V_{c,max}$ and J_{max} collected across a wide range of environmental gradients (Ali et al., 2015). After model fitting, a sensitivity analysis was performed to gauge the response of the

model to parametric variation and to environmental drivers (temperature, photosynthetic active radiation, day length, relative humidity and atmospheric CO_2 concentration). Finally, using climate projections from the Community Climate System Model (CCSM), mean summer-season V_{cmax25} and J_{max25} and their impacts on net photosynthesis were estimated for the globe.

2.2. Model description

The structure of *LUNA* model is based on Xu et al. ~~(2012)~~(2012), where plant leaf nitrogen is divided into four pools: structural nitrogen, photosynthetic nitrogen, storage nitrogen and respiratory nitrogen. We assume that plants optimize their nitrogen allocation to maximize the net photosynthetic carbon gain, defined as the gross photosynthesis (A) minus the maintenance respiration for photosynthetic enzymes (R_{psn}), under specific environmental conditions and given the leaf nitrogen use strategy determined by four parameters in the *LUNA* model. These four parameters in the model include 1) J_{maxb0} (unitless) specifies baseline proportion of nitrogen allocated for electron transport rate; 2) J_{maxb1} (unitless) determines electron transport rate response to light; 3) $t_{c,j0}$ (unitless) specifies the baseline ratio of Rubisco-limited rate to light-limited rate; and 4) H (unitless) determines electron transport rate response to relative humidity. The model uses area-based leaf nitrogen content and different environmental conditions (temperature, CO_2, radiation, relative humidity and day length) as model inputs and predicts $V_{c,max\ 25}$ and J_{max25} based on the optimal amount of nitrogen allocated to different processes.

It is important to point out that the optimization in LUNA model is a conditional optimization given the plant's nitrogen use strategies built into the model. Thus, it is possible that "optimal" values of $V_{c,max\ 25}$ and J_{max25} predicted by the LUNA model for future climate conditions could have a lower net photosynthetic gain compared to fixed values of $V_{c,max\ 25}$ and J_{max25}, where the plant does not follow the nitrogen use strategies built into the LUNA model. An example is

Formatted: Indent: First line: 0.13"

shown in Fig. S1 where the "optimal" net photosynthetic carbon gain using the nitrogen allocation predicted by LUNA model for the elevated temperature is lower than that using fixed nitrogen allocation predicted for the ambient temperature. A complete description of the LUNA model and the detailed associated optimization algorithms are provided in Appendix A. This optimality approach was introduced and tested by Xu et al. ~~(2012)~~(2012) for only three test cases, and here we assess its fidelity at large spatial scale with improvement to account for large scale variability. ~~Optimal~~Optimality approaches are ~~an~~ important ~~tool of~~tools for land surface models, in that they provide a specific testable hypothesis for plant function ~~(Dewar, 2010; Franklin et al., 2012; Schymanski et al., 2009; Thomas and Williams, 2014)~~(Dewar, 2010; Franklin et al., 2012; Schymanski et al., 2009; Thomas and Williams, 2014).

Formatted: Font: Not Italic

2.3. Data and temperature response *functions*

Details of data collection are stated in Ali *et al*. (2015) . Specifically, we conducted a literature search on Google Scholar to locate publications that included words "$V_{c,max}$" or "J_{max}" and also contained "leaf nitrogen content" , "maximum carboxylation rate" , "maximum electron transport rate" , "leaf mass per area", or "specific leaf area". Individual values of $V_{c,max}$, J_{max}, area-based leaf nitrogen content (LNC_a, g N/m^2 leaf) and leaf mass per unit leaf area (LMA, g dry mass/ m^2 leaf) were then obtained by digitizing data from the literature. We used all of the data from Ali *et al*. (2015) with the exception of one study that collected seasonal data on $V_{c,max}$ and J_{max} during prolonged drought ~~(Xu and Baldocchi, 2003)~~(Xu and Baldocchi, 2003), in view that our model only consider the optimal nitrogen allocation based on the monthly climate conditions but did not consider the potential enzyme deterioration due to long-term droughts. In summary, we used 766 data points for $V_{c,max}$ and 643 data points for J_{max} ranging from tropics to

158 the arctic with a total of 125 species. The data include evergreen and deciduous species from
159 arctic, boreal, temperate and tropical areas from different times of the season and different
160 canopy locations (Fig. S2).

161 To allow comparisons of $V_{c,max}$ and J_{max} data collected at different temperatures, we first
162 standardized data to a common reference temperature (25°C). To do this, we employed
163 temperature response functions (TRFs). Because of issues related to the possibility of
164 acclimation to temperature, the appropriate TRF to use is not yet a matter of scientific agreement
165 ~~(Yamori et al., 2006)~~(Yamori et al., 2006). To test the potential impact of our decision on the
166 outcome of the study, we used two alternative temperature response functions in this study. The
167 first temperature response function (TRF1) used Kattge & Knorr's ~~(2007)~~(2007)'s algorithm,
168 which empirically accounts for the potential for acclimation to growth temperature. Following
169 the Community Land Model version 4.5, the growth temperature is constrained between 11°C
170 and 35°C ~~(Oleson et al., 2013)~~(Oleson et al., 2013) to limit the extent of acclimation to growth
171 temperatures found in the calibration data set. The second temperature response function (TRF2)
172 did not consider change in temperature response coefficients to growth temperature ~~(Kattge and~~
173 ~~Knorr, 2007)~~(Kattge and Knorr, 2007). See Appendix B for details of TRF1 and TRF2.

174 Because the LUNA model is based on the C_3 photosynthetic pathway, in this study, we
175 only consider C_3 species. Typically, plant species are grouped into several simple ~~plant~~
176 ~~functional types (~~PFTs~~)~~ in ESMs because of computational limitations and gaps in the ecological
177 knowledge. In view that the processes considered in *LUNA* model are universal across all C_3
178 species and limited coverage of environmental conditions for individual plant functional types,
179 our *LUNA* model does not differentiate among PFTs for C_3 species. Namely, we have a single
180 model for all C_3 PFTs.

Formatted: Font: Not Italic

2.4. Parameter estimation

The four parameters in the LUNA model are difficult to measure in the field. In this study, we estimate these parameters by fitting out model against observations of $V_{c,max25}$ and J_{max25} data using the Differential Evolution Adaptive Metropolis ($DREAM_{(ZS)}$) method (Vrugt et al., 2008, 2009; Laloy and Vrugt, 2012). We used the $DREAM_{(ZS)}$ algorithm (Vrugt et al., 2008, 2009; Laloy and Vrugt, 2012) to calibrate our model because this method uses differential evolution ~~(Storn and Price, 1997)~~ as genetic algorithm for population evolution with a Metropolis selection rule to decide whether candidate points should replace their parents or not. This simple Markov Chain Monte Carlo (MCMC) method exhibits excellent sampling efficiencies on a wide range of model calibration problems, including multimodal and high-dimensional search problems. A detailed description of $DREAM_{(ZS)}$ appears in Vrugt et al., (2008, 2009) and Laloy and Vrugt (2012) and interested readers are referred to these publications. A simple Gaussian likelihood function (No.4 in $DREAM_{(ZS)}$) was used to compare our model simulations of $V_{c,max25}$ and J_{max25} with their observed counterparts. Examples of convergence of the parameters are presented in Fig. ~~S1~~S3 and ~~S2~~S4.

2.5. Model evaluations

In this study, we considered two statistical metrics to analyze the performance of the LUNA model against the $V_{c,max}$ and J_{max} data. They are the coefficient of determination (r^2) ~~(Whitley et al., 2011)~~(Whitley et al., 2011) and the model efficiency (ME) ~~(Whitley et al., 2011)~~(Whitley et al., 2011). The r^2 is estimated using the linear regression model for observed values versus the predicted values. It measures the proportion of variance in $V_{c,max}$ or J_{max} data explained by the model. The model efficiency is given as

$$\mathrm{ME} = 1 - \frac{\sum(y_i - \hat{y}_i)^2}{\sum(y_i - \bar{y})^2},$$

where y_i are the observations, $\hat{y}_i$ are the model estimates and $\bar{y}$ is the mean of observations. It measures the proportion of variance in the $V_{c,max}$ or J_{max} data explained by the 1:1 line between model predictions and observations ~~(Mayer and Butler, 1993; Medlyn et al., 2005)~~(Mayer and Butler, 1993; Medlyn et al., 2005). The ME can range between 0 and 1, where a ME=1 corresponds to a 'perfect' match between modelled and measured data and a ME=0 indicates that the model predictions are only as accurate as the mean of the measured data.

2.6. Model sensitivity analysis

We conducted two sensitivity analyses of our model to identify the importance of the model parameters and the environmental variables. In the first sensitivity analysis, each value of the model parameter (J_{maxb0}, J_{maxb1}, $t_{c,j0}$, and H) was perturbed, one at a time, by +/-15% of their fitted values, to measure the importance of model parameters to modeled $V_{c,max25}$ and J_{max25}. In the second sensitivity analysis, the environmental variables (day length (hours), daytime radiation (W m^{-2}), temperature (^{o}C), relative humidity (unitless), and carbon dioxide (ppm)) were perturbed, one at a time, by +/-15% of their mean values to identify which environmental variable was most likely to drive modeled $V_{c,max25}$ and J_{max25}.

2.7. Changes in $V_{c,max25}$ and J_{max25} under future climate projections

Global surface temperature by year 2100 (relative to present day) could increases by 3.9°C ~~(Friedlingstein et al., 2014)~~(Friedlingstein et al., 2014), with large variations across different regions of the globe ~~(Raddatz et al., 2007)~~(Raddatz et al., 2007). Given the dependence of photosynthesis on temperature, it is critical to examine how much future photosynthesis is likely to change in different regions. In this study, we aim to investigate the importance of changes in $V_{c,max25}$ and J_{max25} as predicted by the LUNA model to the net photosynthesis rate (A_{net})

estimation in future. The importance is measured by the percentage difference in the estimation of future mean A_{net} for the top canopy leaf layer during the summer season by using $V_{c,max25}$ and J_{max25} estimated for historical climate conditions or the $V_{c,max25}$ and J_{max25} estimated for future climate conditions (See Appendix C for details of A_{net} calculation).

We used Coupled Climate Carbon Cycle Model Intercomparison Project Phase 5 (CMIP5) ~~(Meehl et al., 2000)~~(Meehl et al., 2000) model outputs to obtain projections of the future climate. Climate modelers have developed four representative concentration pathways (RCPs) for the 21st century that correspond to different amounts of greenhouse gas emissions ~~(Taylor et al., 2013)~~(Taylor et al., 2013). In this study, we used the historical and future climate conditions simulated by the CCSM 4.0 model under the emission scenario of RCP8.5, which considers the largest greenhouse gas emissions. We did not consider other models and emission scenarios because our main purpose is to estimate the potential impact of our nitrogen allocation model on photosynthesis estimation but not to do a complete analysis under all CMIP5 output. Specifically, we used ten-year climate conditions between 1995 and 2004 for historical and the ten-year climate conditions between 2090 and 2099 for future. We present optimal $V_{c,max25}$ and J_{max25} predictions for the peak growing season months. Data from the NOAA Earth System Research Laboratory over the years 1950 to 2010 ~~(Riebeek, 2011)~~(Riebeek, 2011) showed that the maximum amount of carbon dioxide drawn out of the atmosphere occurs in August and February by the large land masses of Northern and Southern hemisphere, respectively. As a result, June, July and August months were used in this study as the summer season for Northern hemisphere and December, January and February months were considered as the summer season for the Southern Hemisphere. V_{cmax25} and J_{max25} were predicted using the average values of the

248 climate variables for June, July, August and November, December, January for Northern,
249 Southern hemispheres, respectively.

250 In order to identify the importance of changes in different climate variables (temperature,
251 CO_2, radiation and relative humidity) to modeled changes in $V_{c,max25}$ and J_{max25} in the future, we
252 conducted a third sensitivity analysis ~~of~~to investigate the impact of changes in climate variables
253 on model results. In contrast to the previous two sensitivity analyses that focus on the mean
254 current climate conditions, the purpose of the third sensitivity analysis was to explore the global
255 pattern in sensitivity of $V_{c,max25}$ and J_{max25} to changes in climate variables across different
256 biomes of the globe in the future. Specifically, we measured the importance of changes in a
257 specific climate variable by the difference in $V_{c,max25}$ and J_{max25} predicted by the LUNA model
258 driven by historical values or future values of the specific climate variable of interest with all
259 other climate variables set as their historical values.

260

261 **3. Results**

262 *3.1. Model-data comparison of $V_{c,max25}$ and J_{max25}*

263 The DREAM inversion approach allowed us to estimate the four parameters in our ~~*LNUE*~~LUNA
264 model (Table 1). Using the fitted model parameters, the LUNA model explained 54% of the
265 variance of observed $V_{c,max25}$ across all of the species (Fig. 1a) and 65% of the variance in
266 observed J_{max25} (Fig. 1b) using temperature response function TRF1 (a temperature response
267 function that considered the potential of acclimation to growth temperature). When temperature
268 response function TRF2 (a temperature response function that did not consider change in
269 temperature response coefficients to growth temperature) was used, the LUNA model explained
270 57% of variance in observed $V_{c,max25}$ (Fig. 1c) and 66% of the variance in observed J_{max25} (Fig.

1d) across all of the species. By comparing the model predictions with only the studies that reported seasonal cycles of $V_{c,max25}$ and J_{max25}, we found the model explained 67~~%~~ and 53% of the variance in observed $V_{c,max25}$ and J_{max25}, respectively, when TRF1 was used (see Fig. ~~S3~~S5 a~~-~~, b in the supplementary file). The model explained 67~~%~~ and 54% of the variance in observed $V_{c,max25}$ and J_{max25}, respectively, when TRF2 was used (Fig. ~~S3~~S5 c~~-~~, d).

Our model also performed well for different PFTs. When using TRF1, for herbaceous plants, the LUNA model explained about 57% of the variance in observed $V_{c,max25}$ (Fig. ~~S4a~~S6a). The model explained about 58~~%~~ and 47% of the variance in observed $V_{c,max25}$ for shrubs (Fig. ~~S4b~~S6b) and for trees (Fig. ~~S4c~~S6c), respectively. For the electron transport, the LUNA model explained about 49~~%,~~ 85~~%~~ and 46% of the variances in observed J_{max25} for herbaceous plants (Fig. ~~S4d~~S6d), shrubs (Fig. ~~S4 e~~S6e) and trees (Fig. ~~S4f~~S6f), respectively.

When we used a fixed temperature response curve under different growth temperatures (TRF2), for shrubs, ~~-~~the LUNA model has a slightly higher predictive power~~(~~. It explained about 63% of the variances in observed $V_{c,max25}$ (Fig. ~~S5~~S7 b~~)).~~ Across TRF1 and TRF2, the LUNA model explained similar amount of variance in observed $V_{c,max25}$ for herbaceous and trees (Fig. ~~S5~~S7 a, c). For $J_{max25,}$ the LUNA model explained a similar amount of variability for herbaceous, shrubs and trees for TRF1 (Fig. ~~S4~~S6 d-f) and TRF2 (Fig. ~~S5~~S7 d-f).

3.2. Model sensitivity analysis

Sensitivity analysis of the four model parameters (Table 1) showed that all the four parameters had positive effects on $V_{c,max25}$ (Fig. 2 a, c) and J_{max25} (Fig. 2 b, d) regardless of the temperature response function used. t_{c,j_0} had the strongest effect on $V_{c,max25}$ (Fig. 2 a, c) while J_{maxb0} had the strongest effect on J_{max25} (Fig. 2 b, d). H had little impact on either $V_{c,max25}$ and J_{max25} (Fig. 2 a-d).

294 Sensitivity analysis of the climate variables showed that, under both temperature response
295 functions (TRF1 and TRF2), the key drivers of change in $V_{c,max25}$ were radiation, day length,
296 temperature, CO_2 and relative humidity in order of decreasing importance (Fig. 3 a, c). For
297 J_{max25}, the main drivers of change in J_{max25} were day length, temperature, radiation, relative
298 humidity and CO_2 in order of decreasing importance (Fig. 3 b, d), irrespective of which
299 temperature response functions were used.
300
301 *3.3. Impacts of climate change on $V_{c,max25}$ and J_{max25}*
302 Across the globe, the gradient of $V_{c,max25}$ and J_{max25} is similar irrespective of whether TRF1 or
303 TRF2 was used (Fig. 4 and Fig. ~~S6~~S8). Under historical conditions, regions from higher latitudes
304 are predicted to have relatively high $V_{c,max25}$ and J_{max25} while lower latitudes are predicted to have
305 relatively low $V_{c,max25}$ and J_{max25} (Fig. 4a,c for TRF1; Fig. ~~S6a~~S8a, c for TRF2). Future climatic
306 conditions are likely to decrease $V_{c,max25}$ in many continents mainly due to the predicted increase
307 in temperature and CO_2 concentration (Fig. 4b for TRF1; Fig. ~~S6b~~S8b for TRF2). J_{max25} is
308 predicted to decrease at higher latitudes but slightly increasing at lower latitudes (Fig. 4d for
309 TRF1and Fig. ~~S6b~~S8b for TRF2).
310 Our results showed that $V_{c,max25}$ was most sensitive to CO_2, temperature, radiation and
311 relative humidity in order of decreasing importance (Fig. 5 a-d for TRF1 and Fig. ~~S7a~~S9a-d for
312 TRF2). J_{max25} was most sensitive to temperature, radiation, relative humidity and CO_2 in order of
313 decreasing importance (Fig. 6 a-d for TRF1 and Fig. ~~S8a~~S10a-d for TRF2). Across the globe,
314 temperature had negative impacts on $V_{c,max25}$ when using TRF1 (Fig. 5a); however, $V_{c,max25}$ was
315 found to be increasing at the lower latitudes when using TFR2 (Fig. ~~S7a~~S9a).

Formatted: Subscript
Formatted: Subscript

Our model showed that the future summer-season mean photosynthetic rate at the top leaf layer could be substantially overestimated if we does not consider the acclimation of $V_{c,max25}$ and J_{max25} for the future (i.e., using the $V_{c,max25}$ and J_{max25} estimated for historical climate conditions) (Fig. 7a, b), especially for regions with high temperatures (Fig. ~~S9).~~S11). Compared to the model using TRF1, the overestimation of future summer-season mean photosynthesis rates is much higher than the model using TRF2 (Fig. 7b). ~~–~~The overestimation of total global net photosynthetic rate is 10.1~~%~~ and ~16.3% for TRF1 and TRF2, respectively.

4. Discussion

4.1. Model limitations

The assumption that nitrogen is allocated according to optimality principles explained a large part of variability in $V_{c,max25}$ ~~(approximately (~~55%) and in J_{max25} ~~(approximately (~~65%) at the global scale, regardless of the temperature response functions used. It also ~~well~~ captured well the seasonal cycles and the PFT-specific values of $V_{c,max25}$ and J_{max25} (Fig. ~~S3–5).~~S5-7). It has a much improved fitting to the data compared to a multi-linear regression model using LNC_a and *LMA* as predictors, which only explained ~22% of the variance in observed $V_{c,max25}$ (Fig. S12 a, d) and ~13% of the variance in observed J_{max25} (Fig. S12 b, d) for both temperature response functions. These results suggest that our model is able to capture many of the key components of the drivers ~~of~~for $V_{c,max25}$ and J_{max25} across the globe both in space as well as in time. The remaining portion of uncertainty that cannot be explained by our *LUNA* model could be related to variability within the 125 species considered in this study. There are inherent intraspecific variations in leaf traits (Valladares et al., 2000) and in photosynthetic capacity (Moran et al., 2015). Data availability limited the number of species that can be considered and favored ~~the~~a

universal *LUNA* ~~that we used~~model as separate species normally did not cover a sufficiently large range of environmental conditions~~; however~~. Yet, we should be able to fit our model to specific PFTs when additional data become available ~~that provides more complete~~with a large enough coverage of environmental conditions ~~and PFTs~~. We expect that such a model would be able to describe and capture ~~more~~adequately a larger portion of the variability observed in $V_{c,max25}$ and $J_{max25.}$

Unexplored nutrient limitations and other plant physiological properties could also play a factor in the limitation of our model. For example, the nitrogen use efficiency of tropical plants (typically modest to low nitrogen) can be diminished by low phosphorus (Cernusak et al., 2010; ~~Reich and Oleksyn, 2004~~Reich and Oleksyn, 2004), suggesting that our model could be improved by considering multiple nutrient limitations ~~(Goll et al., 2012; Walker et al., 2014; Wang et al., 2010)~~(Goll et al., 2012; Walker et al., 2014; Wang et al., 2010). Our treatment of photosynthetic capacity could also be improved by incorporating species-specific mesophyll and stomatal conductance ~~(Medlyn et al., 2011)~~(Medlyn et al., 2011), by analyzing leaf properties such as leaf life span ~~(Wright et al., 2004)~~(Wright et al., 2004), or by considering soil nutrient ~~and~~, soil water availability~~.~~, and soil pH (Maire et al., 2015).

Another potential reason why the model is unable to explain a significant part of uncertainty in the observation is due to that fact that the measurement error on $V_{c,max25}$ and J_{max25} is rarely reported in the literature. Measurement errors on $V_{c,max25}$ and J_{max25} could result from many sources. Firstly, through different statistical fitting approaches used to fit the Farquhar et al. model ~~(Dubois et al., 2007; Manter and Kerrigan, 2004)~~(Dubois et al., 2007; Manter and Kerrigan, 2004) to determine the transition C_i value (the value of C_i used to differentiate between Rubisco and RUBP limitations), which are not yet consistent in the literature ~~(Miao et al.,~~

~~2009)~~(Miao et al., 2009). Secondly, obtaining accurate or biologically realistic estimates of dark respiration is often challenging ~~(but see Dubois et al., 2007)~~(but see Dubois et al., 2007), and as such, dark respiration is sometimes not reported ~~(Medlyn et al., 2002b)~~(Medlyn et al., 2002b).

4.2. Importance of environmental control on $V_{c,max25}$ and J_{max25}

Our model predicts that higher temperatures generally lead to lower values of $V_{c,max25}$ and J_{max25} (Fig. 3a, c). As temperature increases, the nitrogen use efficiencies of $V_{c,max}$ and J_{max} also increase and thus plants need a lower amount of nitrogen allocated for carboxylation and electron transport. This is true for all the sites except for $V_{c,max25}$ in the hotter regions when TRF2 was used (Fig. ~~S7a). The reason is because LUNA model will use a higher increase in night-time temperature (e.g., 22 to 30°C) than daytime temperature (e.g., from 31 to 33°C) as constrained by the maximum temperature for optimization in TRF2 (i.e., 33°C). Thus, the nitrogen use efficiency of daily respiration increases much strongly than the nitrogen use efficiency of $V_{c,max}$. Photosynthesis and respiration is balanced within the model, so plants do not need to invest a lot of nitrogen in respiratory enzymes under hot regions. Therefore, more nitrogen is available for other processes, and the proportion of nitrogen allocated to carboxylation and thus $V_{c,max25}$ increased accordingly.~~S9a). The reason is because LUNA model will use a higher increase in night-time temperature (e.g., 22 to 30°C) than daytime temperature (e.g., from 31 to 33°C) , because the daytime temperature is constrained by the maximum temperature for optimization in TRF2 (i.e., 33°C). To maximize the net photosynthetic carbon gain, the model predicts a higher proportion of nitrogen allocated to carboxylation to compensate for a higher nighttime respiration rate. Therefore, the LUNA model predicts a higher value of $V_{c,max25}$. Yet, this may

Formatted: Subscript

Formatted: Subscript

result from the deficiency of TRF2 by not considering thermal acclimation under future global warming (Lombardozzi et al., 2015).

Our model predicts that CO_2 has negligible effects on J_{max25}, which is supported by reports from other studies ~~(e.g. Maroco et al., 2002)~~(e.g. Maroco et al., 2002). A meta-analysis of 12 FACE experiments indicated reductions of J_{max} of approximately 5% but a 10% reduction in $V_{c,max25}$ under elevated CO_2 ~~(Long et al., 2004)~~(Long et al., 2004). Our model also predicts that relative humidity has little effect on $V_{c,max25}$. This may be due to the fact that most of the values of $V_{c,max25}$ and J_{max25} used in our dataset were reported with relatively high humidity values~~. But~~; however, our model~~,~~ may have underestimated the effects of prolonged drought on $V_{c,max25}$ under low humidity conditions ~~(Xu and Baldocchi, 2003)~~(Xu and Baldocchi, 2003), which we did not consider. Under prolonged drought, plants close their stomata and photosynthesis is greatly reduced (Breshears et al., 2008; ~~McDowell, 2011)~~McDowell, 2011). Without carbon input and high temperatures during drought, photosynthetic enzymes may degenerate, which could decrease $V_{c,max25}$ substantially ~~(Limousin et al., 2010; Xu and Baldocchi, 2003)~~(Limousin et al., 2010; Xu and Baldocchi, 2003).

There are many different ways to incorporate environmental controls on $V_{c,max25}$ and J_{max25}. One simple approach is to use empirical statistical models between environmental variables and $V_{c,max25}$ and J_{max25} (e.g. Ali et al., 2015; Verheijen et al., 2013), which has been shown to improve the model simulations (Verheijen et al., 2015). One key limitation of such models is that they may have risk of inaccurate extrapolation under novel future climate conditions. The optimization model such as LUNA could be more reliable in their predictions under novel future climate conditions as they account for the key assumptions that could be robust under different environmental conditions. By far, optimality approaches have been used to predict many

different plant structures and functions under different environmental conditions such as carbon allocations (Franklin et al., 2012), leaf C:N (Thomas and Williams, 2014), root distribution (McMurtrie et al., 2012), and stomata conductance (Cowan and Farquhar, 1977). For the photosynthetic capacity optimization, Haxeltine and Prentice (1996) has used an optimization approach to predict $V_{c,max25}$ based on the trade-off between photosynthesis and respiration, which has been incorporated into land surface models including LPJ-GUESS (Smith et al., 2001) and LPJmL (Sitch et al., 2003). Both LUNA model and the model of Haxeltine and Prentice (1996) considered the $V_{c,max25}$ component and respiration; however, LUNA model is currently only designed for the leaf level while model of Haxeltine and Prentice (1996) is applicable for both the leaf and canopy level. The key improvements of LUNA model include the explicit considerations of other important processes such as light capture and electron transport and 2) the evaluations against global datasets under different environmental conditions.

Formatted: Font: Not Italic, Not Superscript/ Subscript

4.3. Importance of changes in $V_{c,max25}$ and J_{max25} to future photosynthesis estimation

Formatted: Subscript

Formatted: Subscript

Our model suggests that most regions of the world will likely have reductions in $V_{c,max25}$ (Fig. 4b and Fig. ~~S6b~~S8b), because increased temperature (Fig. ~~S10~~S13) coupled with elevated CO_2 will increase nitrogen use efficiency of Rubisco and thus plants are able to reduce the amount of nitrogen allocated for Rubisco to reduce the carbon cost required for enzyme maintenance. Similarly, J_{max25} will also decrease globally, except in regions where the present growing temperatures are high (Fig. ~~S9b~~S12b). The increase of J_{max25} can be attributed to leaf temperature limitation and increased shortwave radiation~~.~~ (Fig. S14 and S15). Temperature will have ~~little~~a small impact on nitrogen allocation in regions with historically high growing season temperatures because leaf temperature in already close to or high than the upper limit of optimal

nitrogen allocation (42°C for TRF1 and 33°C for TRF2). Based on eq. (A11), higher levels of shortwave solar radiation will increase nitrogen allocation to electron transport ~~(Evans and Poorter, 2001)~~(Evans and Poorter, 2001).

If we do not account for the potential acclimation of $V_{c,max25}$ and $V_{c,max25}$ under future climate conditions as predicted by the LUNA model, our analysis indicates that ESM predictions of future global photosynthesis at the uppermost leaf layer will likely be overestimated by as much as 10~~14~~16% if $V_{c,max25}$ and J_{max25} are held fixed (Fig. 7). ~~Therefore~~The higher overestimation for TRF2 (16.3%) than TRF1 (10.1%) could result from the fact that TFR2 does not account for future thermal acclimation and thus the LUNA model predicts a large nitrogen allocation acclimation for future climate change. In both cases, our results suggest that, to reliably predict global plant responses to future climate change, ESMs should incorporate models that use environmental control on $V_{c,max25}$ and J_{max25}. It has been recently suggested that nitrogen-related factors are not well represented in ESMs ~~(Houlton et al., 2015; Wieder et al., 2015)~~(Houlton et al., 2015; Wieder et al., 2015). Our nitrogen partitioning scheme would help alleviate biases into the predictions of future photosynthetic rates, and also climate processes that are dependent on these predictions (Bonan et al., 2011; ~~Knorr and Kattge, 2005~~Knorr and Kattge, 2005; Rogers, 2014).

Field Code Changed

5. Code availability

This LUNA model has been implemented into CLM5.0 which will be openly available after its release in early 2016. Meanwhile, we have codes available in the form of MATLAB, FORTRAN and C#. They can be obtained upon request by sending an email to cxu@lanl.gov.

~~5.~~6. Appendices

Appendix A: *Leaf Utilization of Nitrogen for Assimilation* (*LUNA*) Model

The LUNA model ~~(Xu et al., 2012)~~(Xu et al., 2012) considers nitrogen allocation within a given leaf layer in the canopy that has a predefined leaf-area-based plant leaf nitrogen availability (LNC_a; gN/m^2 leaf) to support its growth and maintenance. The structure of the LUNA model is adapted from Xu et al. ~~(2012)~~(2012), where the plant nitrogen at the leaf level is divided into four pools: structural nitrogen ($N_{str;}$ g N/m^2 leaf), photosynthetic nitrogen ($N_{psn;}$ g N/m^2 leaf), storage nitrogen ($N_{store;}$ g N/m^2 leaf), and respiratory nitrogen ($N_{resp;}$ g N/m^2 leaf). Namely,

$$LNC_a = N_{psn} + N_{str} + N_{store} + N_{resp}. \quad \text{(A1)}$$

The photosynthetic nitrogen, N_{psn} , is further divided into nitrogen for light capture ($N_{lc\ ;}$ g N/m^2 leaf), nitrogen for electron transport ($N_{et;}$ g N/m^2 leaf), and nitrogen for carboxylation ($N_{cb;}$ g N/m^2 leaf). Namely,

$$N_{psn} = N_{et} + N_{cb} + N_{lc}. \quad \text{(A2)}$$

The structural nitrogen, N_{str}, is calculated as the multiplication of leaf mass per unit area (LMA: g biomass/m^2 leaf), and the structural nitrogen content (SNC: ~~gN~~g N/g biomass). Namely,

$$N_{str} = \text{SNC} \cdot \text{LMA}, \quad \text{(A3)}$$

where SNC is set to be fixed at 0.002 (gN/g biomass), based on data on C:N ratio from dead wood ~~(White et al., 2000)~~(White et al., 2000). The functional leaf nitrogen content (FNC_a; gN/m^2 leaf) is defined by subtracting structural nitrogen content, N_{str}, from the total leaf nitrogen content (LNC_a; gN/m^2 leaf),

$$FNC_a = LNC_a - N_{str}. \quad \text{(A4)}$$

We assume that plants optimize their nitrogen allocations (i.e., $N_{store,}$ $N_{resp,}$ N_{lc} , $N_{et,}$ N_{cb}) to maximize the net photosynthetic carbon gain, defined as the gross photosynthesis (A) minus the maintenance respiration for photosynthetic enzymes (R_{psn}), under specific environmental conditions and given plant's strategy of leaf nitrogen use. Namely, the solutions of nitrogen allocations { $N_{store,}$ $N_{resp,}$ N_{lc} , $N_{et,}$ N_{cb} } can be estimated as follows,

$$\{\hat{N}_{store,}\hat{N}_{resp,}\hat{N}_{lc},\ \hat{N}_{et,}\hat{N}_{cb}\} = \underset{N_{store}+N_{resp}+N_{lc}+N_{et}+N_{cb}<FNC_a}{argmax} (A-R_{psn}). \quad \text{(A5)}$$

The gross photosynthesis, A , was calculated with a coupled leaf gas exchange model based on the Farquhar et al. ~~(1980)~~(1980) model of photosynthesis and Ball-Berry-type stomatal conductance model (Ball et al., 1987) (See Appendix C for details). The maintenance respiration for photosynthetic enzymes, R_{psn}, is calculated by the multiplication of total photosynthetic nitrogen (N_{psn}) and the maintenance respiration cost for photosynthetic enzyme (NUE_{rp}, see Appendix D). Namely,

$$R_{psn} = NUE_{rp}N_{psn}. \quad \text{(A6)}$$

In the LUNA model, the maximum electron transport rate (J_{max}; μmol electron m^{-2} s^{-1}) is simulated to have a baseline allocation of nitrogen and additional nitrogen allocation to change depending on the average daytime photosynthetic active radiation (PAR; μmol electron m^{-2} s^{-1}), day length (hours) and air humidity. Specifically, we have

$$J_{max} = J_{max0} + J_{maxb1}f(day\ length)f(humidity)\alpha\ PAR. \quad \text{(A7)}$$

The baseline electron transport rate, J_{max0}, is calculated as follows,

$$J_{max0} = J_{maxb0}FNC_aNUE_{J_{max}} \quad \text{(A8)}$$

where J_{maxb0} (unitless) is the baseline proportion of nitrogen allocated for electron transport rate. $NUE_{J_{max}}$ (μmol electron s^{-1} g^{-1}N) is the nitrogen use efficiency of J_{max} (see eq. (D2) for details). J_{maxb1} (unitless) is a coefficient determining the response of the electron transport rate to amount of absorbed light ($i.e., \alpha PAR$). $f(day\ length)$ is a function specifies the impact of day length (hours) on J_{max} in view that longer day length has been demonstrated by previous studies to alter $V_{c,max25}$ and J_{max25} (Bauerle et al., 2012; Comstock and Ehleringer, 1986) through photoperiod sensing and regulation ~~(e.g. Song et al., 2013)~~(e.g. Song et al., 2013). Following Bauerle et al. (2012), $f(day\ length)$ is simulated as follows,

$$f(day\ length) = \left(\frac{day\ length}{12}\right)^2. \quad \text{(A9)}$$

$f(humidity)$ represents the impact of air humitidy on J_{max}. We assume that higher humidity leads to higher J_{max} with less water limiation on stomta opening and that low relative humidity has a stronger impact on nitrogen allocation due to greater water limitation. When relative humidity (RH; unitless) is too low, we assume that plants are physiologically unable to reallocate nitrogen. We therefore assume that there exists a critical value of relative humidity (RH_0 = 0.25; unitless), below which there is no optimal nitrogen allocation. Based on the above assumptions, we have

$$f(humidity) = \left(1 - e^{\left(-H\frac{\max(RH-RH_0,\,0)}{1-RH_0}\right)}\right), \quad \text{(A10)}$$

where H (unitless) specifies the impact of relative humidity on electron transport rate. Replacing eq. (A7) with eqs. (A 8), (A9) and (A10), we have

$$J_{max} = J_{maxb0} FNC_a NUE_{J_{max}} + J_{maxb1}\left(\frac{day\ length}{12}\right)^2\left(1 - e^{\left(-H\frac{\max(RH-RH_0,0)}{1-RH_0}\right)}\right)\alpha\ \text{PAR}. \quad \text{(A11)}$$

The efficiency of light energy absorption (unitless), α, is calculated depending on the amount of nitrogen allocated for light capture, N_{lc}. Following Niinemets and Tenhunen ~~(1997)~~(1997), we have,

$$\alpha = \frac{0.292}{1+\frac{0.076}{N_{lc}C_b}}, \quad \text{(A12)}$$

where 0.292 is the conversion factor from photon to electron. C_b is the conversion factor (1.78) from nitrogen to chlorophyll. After we estimate J_{max} , the actual electron transport rate with the daily maximum radiation (J_x) can be calculated using the empirical expression of Smith ~~(1937)~~(1937),

$$J_x = \frac{\alpha PAR_{max}}{\left(1+\frac{\alpha^2 PAR_{max}{}^2}{Jmax^2}\right)^{0.5}}, \quad \text{(A13)}$$

where PAR_{max} (μmol m^{-2} s^{-1}) is the maximum photosynthetically active radiation during the day.

Based on Farquhar et al. ~~(1980)~~(1980) and Wullschleger ~~(1993)~~(1993), we can calculate the electron-limited photosynthetic rate under daily maximum radiation (W_{jx}) and the Rubisco-limited photosynthetic rate (W_c) as follows,

$$W_{J_x} = K_j J_x, \quad \text{(A14)}$$

$$W_c = K_c V_{c,max}, \quad \text{(A15)}$$

where K_j and K_c as the conversion factors for J_x, $V_{c,max}$ ($V_{c,max}$ to W_c and J_x to W_{J_x}), respectively [see eqs. (C4) and (C6) in Appendix C for details of calculation]. Based on Xu et al. ~~(2012)~~(2012), Maire et al. ~~(2012)~~(2012) and Walker et al. ~~(2014), we assume that W_c is proportional to W_{J_x}.~~(2014), we assume that W_c is proportional to W_{J_x}. Specifically, we have

$$W_c = t_{c,j} W_{J_x}, \quad \text{(A16)}$$

where $t_{c,j}$ is the ratio of W_c to W_{J_x}. We recognize that this ratio may change depending on the nitrogen use efficiency of carboxylation and electron transport (Ainsworth and Rogers, 2007) and therefore introduce the modification as follows,

$$t_{c,j} = t_{c,j_0} \left(\frac{NUE_c / NUE_j}{NUE_{c0} / NUE_{j0}} \right)^{0.5}, \quad \text{(A17)}$$

where t_{c,j_0} (unitless) is the ratio of Rubisco limited rate to light limited rate, NUE_{c0} (μmol CO_2 s^{-1} $g^{-1}N$), NUE_{j0} (μmol CO_2 s^{-1} $g^{-1}N$) are the daily nitrogen use efficiency of W_c and W_j under reference climate conditions defined as the 25°C leaf temperature and atmospheric CO_2 concentration of 380 ppm, with leaf internal CO_2 concentration set as 70% of the atmospheric CO_2 concentration. NUE_c (μmol CO_2 s^{-1} $g^{-1}N$), NUE_j (μmol CO_2 s^{-1} $g^{-1}N$) are the nitrogen use efficiency of W_c and W_j at the current climate conditions. See eqs (D6) and (D7) for details of calculation. The term $\frac{NUE_c / NUE_j}{NUE_{c0} / NUE_{j0}}$ determines that the higher nitrogen use efficiency of W_c compared to that of W_j will lead to a higher value of $t_{c,j}$ (or a higher value of W_c given the same value of W_j). The exponent 0.5 was used to ensure that the response of $V_{c,max}$ to elevated CO_2 is down-regulated by approximately 10% when CO_2 increased from 365 ppm to 567 ppm as reported by Ainsworth & Rogers (2007).

Replacing eq. (A16) with eqs. (A14), (A15) and (A17) , we are able to estimate the maximum carboxylation rate ($V_{c,max}$; μmol CO_2 m^{-2} s^{-1}) as follows,

$$V_{c,max} = t_{c,j_0} \left(\frac{NUE_c / NUE_j}{NUE_{c0} / NUE_{j0}} \right)^{0.5} \left(\frac{K_j}{K_c} \right) J_x. \quad \text{(A18)}$$

Following Collatz et al. (1991a), the total respiration (R_t) is calculated in proportion to $V_{c,max}$,

$$R_t = 0.015 V_{c,max}. \quad \text{(A19)}$$

Accounting for the daytime and nighttime temperature, we are able to estimate the daily respirations as follows,

$$R_{td} = \mathrm{R_t}[D_{day} + D_{night} f_r(T_{night})/f_r(T_{day})] , \quad \text{(A20)}$$

where D_{day} and D_{night} are daytime and nighttime durations in seconds. $f_r(T_{night})$ and $f_r(T_{day})$ are the temperature response functions for respiration (see eq. (B1) for details).

In summary, given an initial estimation of N_{lc}, we are able to first estimate the efficiency of light energy absorption α using eq. (A12). With that, we are able to estimate the maximum electron transport rate , J_{max}, using eq. (A11). The nitrogen allocated for electron transport can thus be calculated as follows,

$$N_{et} = \frac{Jmax}{NUE_{Jmax}} . \quad \text{(A21)}$$

Then, based on eq. (A18), we are able to estimate the corresponding the maximum carboxylation rate $V_{c,max}$ and the nitrogen allocated for carboxylation as follows,

$$N_{cb} = \frac{V_{c,max}}{NUE_{Vc,max}} \quad \text{(A22)}$$

where $NUE_{Vc,max}$ is the nitrogen use efficiency for $V_{c,max}$. See eq. (D1) for details of calculation. Using eq. (A 20), we are able to estimate R_{td} and thus the nitrogen allocated for respiration as follows,

$$N_{resp} = \frac{R_{td}}{NUE_r} , \quad \text{(A23)}$$

where NUE_r is nitrogen use efficiency of enzymes for respiration. See eq. (D3) for details of calculation. Finally, the "storage" nitrogen is calculated as follows,

$$N_{store} = FNC_a - N_{resp} - N_{cb} - N_{lc} - N_{et}. \quad \text{(A24)}$$

Note that this "storage" nitrogen is mainly a remaining component of FNC_a. Its formulation is different from the formulation of Xu et al ~~(2012)~~(2012) where N_{store} is set as a linear function of net photosynthetic rate. This modification is based on the observations that the preliminary fitting to data using the linear function shows no dependence of N_{store} on net photosynthetic

rate. To make the solutions realistic, we set minimum of N_{store} as 5% of NC_a in view of potential nitrogen for plant functionality that is not accounted for by photosynthesis and respiration. By exploring different values of nitrogen allocated for light capture N_{lc} and using the eqs. (A21-23), we will find the "optimal" nitrogen allocations (~~$\hat{N}_{store,}\hat{N}_{resp,}\hat{N}_{lc}$, $\hat{N}_{et,}\hat{N}_{cb}$~~ $\hat{N}_{store,}\hat{N}_{resp,}\hat{N}_{lc}$, $\hat{N}_{et,}\hat{N}_{cb}$) until the net photosynthetic rate is maximized (see eq. (A5)) given a specific set of nitrogen allocation coefficients (i.e., J_{maxb0}, J_{maxb1}, H, and t_{c,j_0}). The detailed optimization algorithms are implemented as follows:

1) Increase the nitrogen allocated (N_{lc}) for light capture (from a small initial value of 0.05) and calculate the corresponding light absorption rate α with eq. (A12);
2) Calculate J_{max} from eq. (A11) and derive the nitrogen allocated to electron transport, N_{et}, using eq. (A21);
3) Calculate $V_{c,max}$ from eq. (A18) and derive the nitrogen allocated to Rubisco, N_{cb}, using eq. (A22);
4) Calculate the total respiration R_{td} from eq. (A20) and derive the nitrogen allocated to respiration, N_{resp}, using eq. (A23);
5) Calculate the total nitrogen invest in photosynthetic enzymes including nitrogen for electron transport, carboxylation and light capture using eq. (A2);
6) Calculate the gross photosynthetic rate, A, and the maintenance respiration for photosynthetic enzymes, R_{psn}, by eq. (A6);
7) Repeat steps 1) to 6) until the increase from previous time step in A is smaller than or equal to the increase in R_{psn}.

Since the response of $V_{c,max}$ and J_{max} to increasing temperature shows a steady rise to an optimum followed by a relatively rapid decline (Bernacchi et al., 2003~~; Kattge and Knorr, 2007;~~

~~Leuning, 2002; Medlyn et al., 2002a)~~; Kattge and Knorr, 2007; Leuning, 2002; Medlyn et al., 2002a), we postulate that the detrimental heat stress on leaf enzymatic activity beyond this optimum ~~(Crafts-Brandner and Law, 2000; Crafts-Brandner and Salvucci, 2000; Law and Crafts-Brandner, 1999; Spreitzer and Salvucci, 2002)~~(Crafts-Brandner and Law, 2000; Crafts-Brandner and Salvucci, 2000; Law and Crafts-Brandner, 1999; Spreitzer and Salvucci, 2002) will cause the leaf to fail to optimize its nitrogen allocation. Consequently, we hypothesized that plants only optimize nitrogen allocation up to their optimum enzymatic activity, which is 42°C for TRF1 and 33°C for TRF2. Regardless of whether plants acclimate to temperature or not, we assume that they do not optimally allocate nitrogen when leaf temperature is below 5°C because low temperatures could substantially limit plant enzymes ~~(Martin et al., 1978; Öquist et al., 1980; Strand and Öquist, 1988)~~(Martin et al., 1978; Öquist et al., 1980; Strand and Öquist, 1988).

After we get the optimal nitrogen allocations ($\hat{N}_{store}, \hat{N}_{resp}, \hat{N}_{lc}, \hat{N}_{et}, \hat{N}_{cb}$ ~~$\hat{N}_{store}, \hat{N}_{resp}, \hat{N}_{lc}, \hat{N}_{et}, \hat{N}_{cb}$~~), we are able to estimate the $V_{c,max25}$ and J_{max25} by rearranging eqs. (~~A20~~A21) and (~~A21~~A22) as follows,

~~$V_{c,\max 25} = \hat{N}_{cb} NUE_{Vc,max25}$~~ $V_{c,\max 25} = \hat{N}_{cb} NUE_{Vc,max25}$

(A25)

~~$J_{\max 25} = \hat{N}_{cb} NUE_{Jmax25}$~~ $J_{\max 25} = \hat{N}_{cb} NUE_{Jmax25}$

(A26)

where ~~$NUE_{Vc,max25}$~~ $NUE_{Vc,max25}$ and ~~NUE_{Jmax25}~~ NUE_{Jmax25} are the nitrogen use efficiency for $V_{c,max25}$ and J_{max25}. See eqs. (D1) and (D2) in Appendix D for details of calculations.

Appendix B: Temperature response functions

Temperature dependence of Rubisco & respiration

The temperature dependence of Rubisco kinetic parameters (K_c, K_o, τ) and mitochondrial respiration in light (R_d) ~~(Farquhar et al., 1980)~~(Farquhar et al., 1980) was an Arrhenius function taken from Bernacchi et al. (2001). The temperature response functions of Rubisco kinetic parameters used are outlined below, which were the same irrespective of whether plants were assumed to acclimate to growth temperatures (Temperature response function one; TRF1) or not (Temperature response function two; TRF2).

Community land model version 4.5 (CLM4.5) ~~(Oleson et al., 2013)~~(Oleson et al., 2013) uses the partial pressures of oxygen, O as 20900Pa. The kinetic properties of Rubisco which depend on temperature are Rubisco specific factor, τ ~~(Jordan and Ogren, 1984)~~(Jordan and Ogren, 1984), K_{cc} and K_o, which are the Michaelis-Menten constants for CO_2 and O_2, respectively. The temperature response function of R_d and kinetic properties of Rubisco (K_{cc}, K_o, τ) are described below, where the fixed coefficients of the equations are values at 25°C.

$$f_r(T_1) = e^{[(46390/RT_0)(1-T_0/T_1)]} \quad \text{(B1)}$$

$$K_0(T_1) = 27840e^{[(36380/RT_0)(1-T_0/T_1)]} \quad \text{(B2)}$$

$$K_c(T_1) = 40.49e^{[(79430/RT_0)(1-T_0/T_1)]} \quad \text{(B3)}$$

$$\tau(T_1) = 2407.834e^{[(37830/RT_0)(1-T_0/T_1)]} \quad \text{(B4)}$$

In the above equations, R is the universal gas constant (8.314 J mol^{-1} K^{-1}), T_l is the leaf temperature (K) and the reference temperature, $T_0 = 298.15K$.

Temperature dependence of $V_{c,max}$ and J_{max}

Temperature sensitivities of $V_{c,max}$ and J_{max} were simulated using a modified Arrhenius function ~~(e.g. Kattge and Knorr, 2007; Medlyn et al., 2002a; Walker et al., 2014)~~(e.g. Kattge and

Knorr, 2007; Medlyn et al., 2002a; Walker et al., 2014). Because the temperature relationship could acclimate, we examined Kattge & Knorr ~~(2007)~~(2007)'s formulation of with and without temperature acclimation to plant growth temperature. We used two temperature dependence functions of $V_{c,max}$ and J_{max}, which are described below.

Temperature response function one (TRF1)

Fundamentally, TRF1 is a temperature dependence of $V_{c,max}$ and J_{max} , which is based on the formulation and parameterization as in Medlyn et al. ~~(2002a)~~(2002a) but further modified by Kattge & Knorr (2007) to make the temperature optima a function of growth temperature (T_g; °C).

Field Code Changed

$$V_{c,max}(T_1, T_g) = V_{c,max25} f_{V_{c,max}}(T_1, T_g) \quad \text{(B5)}$$

with

$$f_{V_{c,max}}(T_1, T_g) = \frac{\left(1+e^{[(S_v T_0 - H_d)/(RT_0)]}\right) e^{[(H_a/RT_0)(1-T_0/T_1)]}}{1+e^{[(S_v T_1 - H_d)/(RT_1)]}} \quad \text{(B6)}$$

where $V_{c,max25}$ is the value of $V_{c,max}$ at the reference temperature ($T_0 = 298.15K$). H_a (J mol^{-1}) is energy of activation and H_d (J mol^{-1}) is the energy of deactivation. The entropy term, S_v (J mol^{-1} K^{-1}), is now a function of temperature ~~(Kattge and Knorr, 2007)~~(Kattge and Knorr, 2007): $S_v = a + bT_g$, where a and b are acclimation parameters for S_v, R is the universal gas constant (8.314 J mol^{-1} K^{-1}) and the leaf temperature is $T_1(K)$.

TRF1 is implemented in CLM4.5 by Oleson et al. ~~(2013)~~(2013), who uses the form of temperature dependence of $V_{c,max}$ and J_{max} as shown in Eq. B5, but with limited temperature acclimation, where $S_v = 668.39 - 1.07 * min(max(tgrowth, 11), 35)$. Other parameters that are present in CLM4.5 model include, H_a = 72000 J mol^{-1} and H_d = 200000 J mol^{-1}. The values of the acclimation parameters (a = 668.39 and b = -1.07) were taken from Table 3 of Kattge &

Knorr ~~(2007)~~(2007), which were fixed across our data set. The same values of a and b are used by CLM4.5.

A equation similar to eq. (B6), $f_{J_{max}}(T_1, T_g)$, is used to describe the temperature dependence of J_{max} with the corresponding S_v equation (that considers limited temperature acclimation). The corresponding values of the acclimation parameters (a and b), were again taken from Table 3 of Kattge & Knorr ~~(2007)~~(2007) and were fixed across our data set. The same values of a and b are used by CLM4.5. We used the remaining parameter values as in CLM4.5 that included, H_a = 50000 J mol^{-1} and H_d = 200000 J mol^{-1}.

Temperature response function two (TRF2)

TRF2 does not consider temperature acclimation. The formulation of TRF2 is same as TRF1 except that in TRF2, the entropy term; S_v (J mol^{-1} K^{-1}) is fixed across our data set. The values of S_v were taken from Table 3 of Kattge & Knorr ~~(2007)~~(2007), which were fixed across our data set. For $V_{c,max25}$, S_v was 649.12 J mol^{-1} K^{-1}, and for J_{max25}, S_v was 646.22 J mol^{-1} K^{-1}.

Appendix C: The Farquhar Photosynthesis & Ball-Berry model

Overview

Photosynthesis is described using a system of three equations and three unknown variables. The three unknown variables include 1) the net rate of leaf photosynthesis (A); 2) the stomatal conductance (g_s); and 3) the intercellular partial pressure of CO_2 (C_i). All of the unknown variables influence one another. The three equations include 1) the Farquhar's non-linear equation (A vs C_i); 2) the Ball–Berry equation (g_s vs A); and 3) the diffusion equation ($A = g_s (C_a - C_i)$). We solved all of these equations simultaneously by taking an iterative approach (Collatz et al., 1991a; ~~Harley et al., 1992~~Harley et al., 1992; ~~Leuning, 1990~~Leuning, 1990). The detailed algorithm for modeling photosynthesis is described below.

Modelling Photosynthesis

The photosynthetic rate (A) depends upon (*i*) the amount, activity, and kinetic properties of Rubisco, and (*ii*) the rate of ribulose-l,5 bisphosphate (RuBP) regeneration via electron transport ~~(Farquhar et al., 1980)~~(Farquhar et al., 1980). The 'minimum' of these two limiting conditions yields the following expression,

$$A = \min(W_c, W_j) \qquad \text{(C2)}$$

where W_c is the Rubisco limited rate and W_j is the electron transport limited rate. The Rubisco-limited carboxylation can be described by,

$$W_c = K_c V_{c,max} \ , \qquad \text{(C3)}$$

with

$$K_c = \frac{\max(0,\ C_i - \frac{0.5O}{\tau})}{C_i + K_{cc}\left(1 + {}^{O}/_{K_o}\right)} \ , \qquad \text{(C4)}$$

where $V_{c,max}$ is the maximum rate of carboxylation, competitive with respect to both CO_2 and oxygen, and K_{cc} and K_o are Michaelis constants for carboxylation and oxygenation, respectively.

τ is the specificity factor for Rubisco ~~(Jordan and Ogren, 1984)~~(Jordan and Ogren, 1984), while C_i, and O are the partial pressures of CO_2 and O_2 in the intercellular air space, respectively. Likewise, the electron-limited rate of carboxylation can be expressed by,

$$W_j = K_j J \ , \qquad \text{(C5)}$$

with

$$K_j = \frac{\max(0, C_i - \frac{0.5O}{\tau})}{4\left(C_i + 2\frac{0.5O}{\tau}\right)}, \qquad \text{(C6)}$$

where J is the potential rate of electron transport, and the factor 4 indicates that the transport of four electrons will generate sufficient ATP and NADPH for the regeneration of RuBP in the Calvin cycle ~~(Farquhar and von Caemmerer, 1982)~~(Farquhar and von Caemmerer, 1982). The potential rate of electron transport is dependent upon irradiance, I, according to the empirical expression of Smith (1937),

$$J = \frac{\alpha I}{\left(1 + \frac{\alpha^2 I^2}{Jmax^2}\right)^{1/2}} \qquad \text{(C7)}$$

where α, the efficiency of light energy conversion is considered as 0.292 (unitless) (Niinemets and Tenhunen, 1997) and J_{max} *is* the maximum rate of electron transport.

Ball-Berry Model

The stomatal conductance (g, m/s) was evaluated by the Ball-Berry empirical stomatal conductance model (Ball et al., 1987):

$$g = g_0 + m\frac{A\ \mathrm{RH}}{C_a} \qquad \text{(C8)}$$

where RH is the relative humidity (unitless) at the leaf surface, C_a is the CO_2 concentration at the leaf surface, and g_0 (0.0005 s/m) and m are the maximum stomatal conductance and slope (9, constant across all C_3 species), respectively.

Field Code Changed

Field Code Changed

The estimation of A could be sensitive to the choice of maximum stomatal conductance slope, which we set the same for all species, despite the evidence that this parameter varies both within and across species ~~(Harley and Baldocchi, 1995; Wilson et al., 2001)~~(Harley and Baldocchi, 1995; Wilson et al., 2001). A recent synthesis provides the first analysis of the global variation in stomatal slope based on an alternative algorithm that considers representation of optimal stomatal behavior ~~(Lin et al., 2015)~~(Lin et al., 2015). However, following CLM4.5, which uses the Ball-Berry empirical stomatal conductance model (Ball et al., 1987), we fixed the value of stomatal slope (m) as 9 for all PFTs in our study.

Calculation of photosynthesis and stomata conductance

We solved Farquhar's non-linear equation (A vs C_i), the Ball-Berry equation (g_s vs A) and the diffusion equation ($A = g_s (C_a - C_i)$ simultaneously by taking an iterative approach (Collatz et al., 1991a; ~~Harley et al., 1992~~Harley et al., 1992; ~~Leuning, 1990~~Leuning, 1990) until values of A, g_s, and C_i were obtained. The three equations were solved in two phases; the first phase included solving the equations for which Rubisco was limiting while the second phase considered light limitation. The following steps were followed:

1) Given the initial values of C_i (where initial value of C_i was assumed 0.7 x ambient CO_2 concentration), the temperature dependence functions of $V_{c,max}$ and J_{max} (see Appendix B), and the temperature dependence of Rubisco kinetics (O, τ, K_c and K_o, Appendix B), A was calculated from equation (C2).
2) CO_2 concentration at the leaf surface (C_a) was determined by calculating the difference between C_i and the partial pressure due to A, wind speed and the dimension of the leaf.
3) Given A and C_a, and using equation C8, stomatal conductance (g) was determined.

4) C_i was determined by calculating the difference between C_a and partial pressure due to A and boundary conditions of the stomata.

5) Using the leaf energy balance based on absorbed short-wave radiation, molar latent heat content of water vapor, air temperature, and a parameter that governs the rate of convective cooling (38.4 J m^{-2} s^{-1} K^{-1}) ~~(Jarvis, 1986; Moorcroft et al., 2001)~~(Jarvis, 1986; Moorcroft et al., 2001), leaf temperature was calculated.

The above five steps were repeated in a systematic way until g was equilibrated. The final value of A was then recorded.

Appendix D: Nitrogen use efficiencies

The nitrogen use efficiency for $V_{c,max}$ (~~$NUE_{V_{c,\max}}$~~ $NUE_{V_{c,\max}}$, μmol CO_2 g^{-1} N s^{-1}) is estimated from a baseline nitrogen use efficiency 25°C (~~$NUE_{V_{c,\max 25}}$~~ $NUE_{V_{c,\max 25}}$) and a corresponding temperature response function at as follows,

$$\text{~~}NUE_{V_{c,\max}} = NUE_{V_{c,\max 25}} \times f_{V_{c,max}}(T, T_g)\text{~~}\ NUE_{V_{c,\max}} = NUE_{V_{c,\max 25}} \times f_{V_{c,max}}(T, T_g), \quad \text{(D1)}$$

with

$$\text{~~}NUE_{V_{c,\max 25}} = 47.3 \times 6.25\text{~~}\ NUE_{V_{c,\max 25}} = 47.3 \times 6.25,$$

where the constant 47.3 is the specific Rubisco activity (μmol CO_2 g^{-1} Rubisco s^{-1}) measured at 25°C and the constant 6.25 is the nitrogen binding factor for Rubisco (*g* Rubisco g^{-1} N) ~~(Rogers, 2014)~~(Rogers, 2014) . ~~$f_{V_{c,max}}(T, T_g)$~~ $f_{V_{c,max}}(T, T_g)$ is the function specifying the temperature dependence of~~$V_{c,max}$~~ $V_{c,max}$ with ~~T~~ T as the leaf temperature () and ~~T_g~~ T_g as the growth air temperature (See Appendix B for details of the temperature dependence of~~$V_{c,max}$~~ $V_{c,max}$).

The nitrogen use efficiency for J_{max} (~~$NUE_{J_{max}}$~~ $NUE_{J_{max}}$, μmol electron g^{-1} N s^{-1}) is estimated based on a characteristic protein cytochrome *f*~~(Evans and Poorter, 2001)~~(Evans and Poorter, 2001),

$$\text{~~}NUE_{J_{max}} = NUE_{J_{max25}} \times f_{Jmax}(T, T_g)\text{~~}\ NUE_{J_{max}} = NUE_{J_{max25}} \times f_{Jmax}(T, T_g), \quad \text{(D2)}$$

779 with

780 $$NUE_{J_{max25}} = 8.06 \times 156 \quad NUE_{J_{max25}} = 8.06 \times 156 ,$$

781 where the coefficient 156 is the maximum electron transport rate for cytochrome *f* at 25°C(μmol
782 electron/μmol cytochrome *f*); 8.06 is the nitrogen binding coefficient for cytochrome *f* (μmol
783 cytochrome *f* g^{-1} N in bioenergetics). $f_{Jmax}(T, T_g)$ $f_{Jmax}(T, T_g)$ is a function specifies the
784 dependence of J_{max} on temperature (See Appendix B for details of the temperature dependence
785 of J_{max}).

786 The nitrogen use efficiency of enzymes for respiration (μmol CO_2 g^{-1}N day^{-1}), NUE_r
787 NUE_r, is assumed to be temperature-dependent. Specifically, it is calculated as follows,

788 $$NUE_r = 33.69\,[D_{day} f_r(T_{day}) + D_{night} f_r(T_{night})]$$

789 $$NUE_r = 33.69\,[D_{day} f_r(T_{day}) + D_{night} f_r(T_{night})] \qquad \text{(D3)}$$

790 where 33.69 is the specific nitrogen use efficiency for respiration at 25°C (μmol CO_2 g^{-1} N s^{-1})
791 (Makino and Osmond, 1991) and $f_r(T)$ specifies the dependence of respiration on temperature.
792 D_{day} and D_{night} is the daytime and nighttime length in seconds.

793 where 33.69 is the specific nitrogen use efficiency for respiration at 25°C (μmol CO_2 g^{-1} N s^{-1})
794 (Makino and Osmond, 1991) and $f_r(T)$ specifies the dependence of respiration on temperature.
795 D_{day} and D_{night} is the daytime and nighttime length in seconds.

796 The maintenance respiration cost for all photosynthetic enzymes (NUE_{rp}, μmol CO_2 g^{-1}N
797 s^{-1}) is calculated as follows:

798 ~~$NUE_{rp} = NUE_{rp25} f_r(T,T_g),$~~ $NUE_{rp} = NUE_{rp25} f_r(T,T_g),$

799 (D4)

800 where ~~NUE_{rp25}~~ NUE_{rp25} is the nitrogen use efficiency at 25 ^{o}C . ~~NUE_{rp25}~~ NUE_{rp25} is estimated

801 from the observation of J_{max25} and $V_{c,max25}$ as follows,

802 ~~$NUE_{rp25} = \frac{0.8 \times 0.5 \times 0.015 \times V_{c,\max 25}}{\frac{J_{\max 25}}{NUE_{J_{max25}}} + \frac{V_{c,\max 25}}{NUE_{V_{c,max25}}} + 0.2}$~~ $NUE_{rp25} = \frac{0.8 \times 0.5 \times 0.015 \times V_{c,\max 25}}{\frac{J_{\max 25}}{NUE_{J_{max25}}} + \frac{V_{c,\max 25}}{NUE_{V_{c,max25}}} + 0.2},$

803 (D5)

804 where the total respiration is set as 1.5% of ~~$V_{c,\max}$ (Collatz et al., 1991b).~~ $V_{c,\max}$ (Collatz et al.,

805 1991b). We assume that 50% of the total respiration is used for maintenance respiration ~~(Van~~

806 ~~Oijen et al., 2010)~~(Van Oijen et al., 2010) and 80% of the maintenance respiration is used for

807 photosynthetic enzyme. In view that the light absorption rate is generally around 80% ~~(Evans~~

808 ~~and Poorter, 2001)~~(Evans and Poorter, 2001), we set the nitrogen for light capture as 0.2 based

809 on eq. (A12) in Appendix A. ~~$NUE_{J_{max25}}$ and $NUE_{V_{c,max25}}$~~ $NUE_{J_{max25}}$ and $NUE_{V_{c,max25}}$ are the nitrogen

810 use efficiency for J_{max25} and $V_{c,max25}$ estimated from eqs. (D1) and (D2). In this study, we used

811 the estimated mean value of 0.715 for ~~NUE_{rp25}~~ NUE_{rp25} based on the data of Ali *et al*. (2015).

812 The nitrogen use efficiency for carboxylation (NUE_c) is calculated as the multiplication

813 of conversion factor K_c and the nitrogen use efficiency for $V_{c,max}$ follows:

814 $$NUE_c = K_c . NUE_{V_{c,max}}, \quad \text{(D6)}$$

where K_c is calculated based on the actual internal CO_2 concentrations and leaf temperature (see eq. (C4) for details). Correspondingly, the reference nitrogen use efficiency for carboxylation (NUE_{c0}) is calculated using the eq. (D5) except that K_c is calculated based on the reference internal CO_2 concentration of 26.95 Pa and the reference leaf temperature of 25°C. The reference internal CO_2 concentration is estimated by assuming 70% of the atmospheric CO_2 concentration of 380 ppm and an air pressure of 101, 325 Pa.

The nitrogen use efficiency for electron transport (NUE_j) is calculated as the multiplication of conversion factor K_j and the nitrogen use efficiency for J_{max} follows:

$$NUE_j = K_j . NUE_{J_{max}}, \quad \text{(D7)}$$

where K_j is calculated based on the actual internal CO_2 concentrations and leaf temperature (see eq. (C6) in Appendix C for details). Correspondingly, the reference nitrogen use efficiency for electron transport (NUE_{j0}) is calculated using the eq. (D6) except that K_j is calculated based on the reference internal CO_2 concentration of 26.95 Pa and the reference leaf temperature of 25°C. The reference internal CO_2 concentration is estimated by assuming 70% of the atmospheric CO_2 concentration of 380 ppm and an air pressure of 101, 325 Pa.

~~6.1.Code availability~~

~~This model is currently implemented into CLM5.0 and will be released to public when CLM 5.0 is released. Meanwhile, we have code available in the form of MATLAB, FORTRAN and C#. It can be obtained upon request by sending an email to exu@lanl.gov.~~

7. Acknowledgements

This work is funded by UC Lab Research Program (ID: 2012UCLRP0IT00000068990) and by the DOE Office of Science, Next Generation Ecosystem Experiment (NGEE)

837 ~~program~~programs in the arctic and in the tropics. This submission is under public release with
838 the approved LA-UR-14-23309.
839

8. References

Ainsworth, E. A. and Rogers, A.: The response of photosynthesis and stomatal conductance to rising (CO_2): mechanisms and environmental interactions, Plant Cell Environment, 30, 258-270, 2007.

Ali, A. A., Xu, C., Rogers, A., McDowell, N. G., Medlyn, B. E., Fisher, R. A., Wullschleger, S. D., Reich, P. B., Vrugt, J. A., Bauerle, W. L., Santiago, L. S., and Wilson, C. J.: Global scale environmental control of plant photosynthetic capacity, Ecological Applications, doi: 10.1890/14-2111.1, 2015. 2015.

Ball, J. T., Woodrow, I. E., and Berry, J. A.: A model predicting stomatal conductance and its contribution to the control of photosynthesis under different environmental conditions., Dordrecht, The Netherlands1987, 221-224.

Bauerle, W. L., Oren, R., Way, D. A., Qian, S. S., Stoy, P. C., Thornton, P. E., Bowden, J. D., Hoffman, F. M., and Reynolds, R. F.: Photoperiodic regulation of the seasonal pattern of photosynthetic capacity and the implications for carbon cycling, PNAS, 109, 8612-8617, 2012.

Bernacchi, C. J., Pimentel, C., and Long, S. P.: *In vivo* temperature response functions of parameters required to model RuBP-limited photosynthesis, Plant, Cell & Environment, 26, 1419-1430, 2003.

Bernacchi, C. J., Singsaas, E. L., Pimentel, C., Portis JR, A. R., and Long, S. P.: Improved temperature response functions for models of Rubisco-limited photosynthesis, Plant, Cell & Environment, 24, 253-259, 2001.

Block, K. and Mauritsen, T.: Forcing and feedback in the MPI-ESM-LR coupled model under abruptly quadrupled CO_2, Journal of Advances in Modeling Earth Systems, 5, 676-691, 2013.

Bonan, G. B., Lawrence, P. J., Oleson, K. W., Levis, S., Jung, M., Reichstein, M., Lawrence, D. M., and Swenson, S. C.: Improving canopy processes in the community land model version 4 (CLM4) using global flux fields empirically inferred from FLUXNET data, Journal of Geophysical Research, 116, 1-22, 2011.

Bonan, G. B., Levis, S., Sitch, S., Vertenstein, M., and Oelson, K. W.: A dynamic global vegetation model for use with climate models: concepts and description of simulated vegetation dynamics, Global Change Biology, 9, 1543-1566, 2003.

Breshears, D. D., Myers, O. B., Meyer, C. W., Barnes, F. J., Zou, C. B., Allen, C. D., McDowell, N. G., and Pockman, W. T.: Tree die-off in response to global change-type drought: mortality insights from a decade of plant water potential measurements, Frontiers in Ecology and the Environment, 7, 185-189, 2008.

Canadell, J. G., Le Quéré, C., Raupach, M. R., Field, C. B., Buitenhuis, E. T., Ciais, P., Conway, T. J., Gillett, N. P., Houghton, R. A., and Marland, G.: Contributions to accelerating atmospheric CO2 growth from economic activity, carbon intensity, and efficiency of natural sinks, ~~Proc Natl Acad Sci U S A~~Proceedings of the National Academy of Sciences, 104, 18866-18870, 2007.

Cernusak, L. A., Winter, K., and Turner, B. L.: Leaf nitrogen to phosphorus ratios of tropical trees: experimental assessment of physiological and environmental controls, New Phytologist, 185, 770-779, 2010.

Collatz, G. J., Ball, J. T., Grivet, C., and Berry, J. A.: Physiological and environmental regualtion of stomatal conductance, photosynthesis, and transpiration: A model that includes a laminar boundary layer, Agricultural and Forest Meteorology, 54, 107-136, 1991a.

Collatz, G. J., Ball, J. T., Grivet, C., and Berry, J. A.: Physiological and environmental regulation of stomatal conductance, photosynthesis and transpiration: a model that includes a laminar boundary layer, ~~Agric For Meteorol~~Agricultural and Forest Meteorology, 54, 107-136, 1991b.

Comstock, J. and Ehleringer, J. R.: Photoperiod and photosynthetic capacity in *Lotus scoparius* Plant, Cell & Environment, 9, 609-612, 1986.

Cowan, I. and Farquhar, G.: Stomatal function in relation to leaf metabolism and environment, 1977, 471-505.

886 Crafts-Brandner, S. J. and Law, R. D.: Effect of heat stress on the inhibition and recovery of ribulose-1,5-
887 bisphosphate carboxylase/oxygenase activation state Planta, 212, 67-74, 2000.
888 Crafts-Brandner, S. J. and Salvucci, M. E.: Rubisco activase constrains the photosynthetic potential of
889 leaves at high temperature and CO_2, PNAS, 97, 2000.
890 Dewar, R. C.: Maximum entropy production and plant optimization theories, Philosophical Transactions
891 of the Royal Society B, 365, 1429-1435, 2010.
892 Dubois, J.-J. B., Fiscus, E. L., Booker, F. L., Flowers, M. D., and Reid, C. D.: Optimizing the statistical
893 estimation of the parameters of the Farquhar–von Caemmerer–Berry model of photosynthesis, New
894 Phytologist, 176, 402-414, 2007.
895 Evans, J. R. and Poorter, H.: Photosynthetic acclimation of plants to growth irradiance: the relative
896 importance of specific leaf area and nitrogen partitioning in maximizing carbon gain, Plant, Cell &
897 Environment, 24, 755-767, 2001.
898 Farquhar, G. D. and von Caemmerer, S. (Eds.): Modelling of photosynthetic response to environmental
899 conditions, Heidelberg-Berlin-New York: Springer-Verlag, 1982.
900 Farquhar, G. D., Von Caemmerer, S., and Berry, J.: A biochemical model of photosynthetic CO_2
901 assimilation in leaves of C_3 species, Planta, 149, 78-90, 1980.
902 Franklin, O., Johansson, J., Dewar, R. C., Dieckmann, U., McMurtrie, R. E., Brännström, Å., and Dybzinski,
903 R.: Modeling carbon allocation in trees: a search for principles, Tree Physiology, 32, 648-666, 2012.
904 Friedlingstein, P., Meinshausen, M., Arora, V. K., Jones, C. D., Anav, A., Liddicoat, S. K., and Knutti, R.:
905 Uncertainties in CMIP5 climate projections due to carbon cycle feedbacks, Journal of Climate, 27, 511-
906 526, 2014.
907 Friend, A.: Use of a model of photosynthesis and leaf microenvironment to predict optimal stomatal
908 conductance and leaf nitrogen partitioning, Plant, Cell & Environment, 14, 895-905, 1991.
909 Goll, D. S., Brovkin, V., Parida, B. R., Reick, C. H., Kattge, J., Reich, P. B., van Bodegom, P. M., and
910 Niinemets, U.: Nutrient limitation reduces land carbon uptake in simulations with a model of combined
911 carbon, nitrogen and phosphorus cycling, Biogeosciences, 9, 3547-3569, 2012.
912 Hanson, P. J., Amthor, J. S., Wullschleger, S. D., Wilson, K. B., Grant, R. F., Hartley, A., Hui, D., Hunt, J. E.
913 R., Johnson, D. W., Kimball, J. S., King, A. W., Luo, Y., McNulty, S. G., Sun, G., Thornton, P. E., Wang, S.,
914 Williams, M., Baldocchi, D. D., and Cushman, R. M.: OAK FOREST CARBON AND WATER SIMULATIONS:
915 MODEL INTERCOMPARISONS AND EVALUATIONS AGAINST INDEPENDENT DATA, Ecological Monographs,
916 74, 443-489, 2004.
917 Harley, P. C. and Baldocchi, D. D.: Scaling carbon dioxide and water vapour exchange from leaf to canopy
918 in a decisuous forest. I. Leaf model parametrization, Plant, Cell & Environment, 18, 1146-1156, 1995.
919 Harley, P. C., Thomas, R. B., Reynolds, J. F., and Strain, B. R.: Modelling photosynthesis of cotton grown
920 in elevated CO_2 Plant, Cell & Environment, 15, 271-282, 1992.
921 Haxeltine, A. and Prentice, I. C.: A general model for the light-use efficiency of primary production,
922 Functional Eocolgy, 10, 551-561, 1996.
923 Houlton, B. Z., Marklein, A. R., and Bai, E.: Representation of nitrogen in climate change forecasts,
924 Nature Clim. Change, 5, 398-401, 2015.
925 Hurrell, J. W., Holland, M. M., Gent, P. R., Ghan, S., Kay, J. E., Kushner, P. J., Lamarque, J. F., Large, W. G.,
926 Lawrence, D., Lindsay, K., Lipscomb, W. H., Long, M. C., Mahowald, N., Marsh, D. R., Neale, R. B., Rasch,
927 P., Vavrus, S., Vertenstein, M., Bader, D., Collins, W. D., Hack, J. J., Kiehl, J., and Marshall, S.: The
928 Community Earth System Model: A Framework for Collaborative Research, Bulletin of the American
929 Meteorological Society, 94, 1339-1360, 2013.
930 Jarvis, P. G.: Coupling of carbon and water interactions in forest stands, Tree Physiology, 2, 347-368,
931 1986.

Jordan, D. B. and Ogren, W. L.: The CO_2/O_2 specificity of ribulose 1,5-biphosphate carboxylase/oxygenase. Dependence on ribulose-biphosphate concentration, pH and temperature, Planta, 161, 308-313, 1984.
Kattge, J. and Knorr, W.: Temperature acclimation in a biochemical model of photosynthesis: a reanalysis of data from 36 species, Plant, Cell & Environment, 30, 1176-1190, 2007.
Kattge, J., Knorr, W., Raddatz, T., and Wirth, C.: Quantifying photosynthetic capacity and its relationship to leaf nitrogen content for global-scale terrestrial biosphere models, Global Change Biology, 15, 976-991, 2009.
Knorr, W. and Kattge, J.: Inversion of terrestrial ecosystem model parameter values against eddy covariance measurements by Monte Carlo sampling, Global Change Biology, 11, 1333-1351, 2005.
Laloy, E. and Vrugt, J. A.: High-dimensional posterior exploration of hydroligic models using multiple-try DREAM($_{zs}$) and high-performance computing, Water Resources Research, 48, W01526, 2012.
Law, R. D. and Crafts-Brandner, S. J.: Inhibition and acclimation of photosynthesis to heat stress is closely correlated with activation of ribulose-1,5-bisphosphate carboxylase/ oxygenase, Plant Physiology, 120, 173-181, 1999.
Leuning, R.: Modeling stomatal behavior and photosynthesis of *Eucalyptus grandis*, Australian Journal of Plant Physiology, 17, 159-175, 1990.
Leuning, R.: Scaling to a common temperature improves the correlation between photosynthesis parameters J_{max} and V_{cmax}, Journal of Experimental Botany, 307, 345-347, 1997.
Leuning, R.: Temperature dependence of two parameters in a photosynthesis model, Plant, Cell & Environment, 25, 1205-1210, 2002.
Limousin, J.-M., Misson, L., Lavoir, A.-V., Martin, N. K., and Rambal, S.: Do photosynthetic limitations of evergreen Quercus ilex leaves change with long-term increased drought severity?, Plant, Cell & Environment, 33, 863-875, 2010.
Lin, Y.-S., Medlyn, B. E., Duursma, R. A., Prentice, I. C., Wang, H., Baig, S., Eamus, D., de Dios, V. R., Mitchell, P., Ellsworth, D. S., de Beeck, M. O., Wallin, G., Uddling, J., Tarvainen, L., Linderson, M.-L., Cernusak, L. A., Nippert, J. B., Ocheltree, T. W., Tissue, D. T., Martin-StPaul, N. K., Rogers, A., Warren, J. M., De Angelis, P., Hikosaka, K., Han, Q., Onoda, Y., Gimeno, T. E., Barton, C. V. M., Bennie, J., Bonal, D., Bosc, A., Low, M., Macinins-Ng, C., Rey, A., Rowland, L., Setterfield, S. A., Tausz-Posch, S., Zaragoza-Castells, J., Broadmeadow, M. S. J., Drake, J. E., Freeman, M., Ghannoum, O., Hutley, L. B., Kelly, J. W., Kikuzawa, K., Kolari, P., Koyama, K., Limousin, J.-M., Meir, P., Lola da Costa, A. C., Mikkelsen, T. N., Salinas, N., Sun, W., and Wingate, L.: Optimal stomatal behaviour around the world, Nature Clim. Change, advance online publication, 2015.
Lombardozzi, D. L., Bonan, G. B., Smith, N. G., Dukes, J. S., and Fisher, R. A.: Temperature acclimation of photosynthesis and respiration: A key uncertainty in the carbon cycle-climate feedback, Geophysical Research Letters, 42, 8624-8631, 2015.
Long, S. P., Ainsworth, E. A., Rogers, A., and Ort, D. R.: Rising atmospheric carbon dioxide: plants FACE the future, Ann. Rev. Plant. Biol, 55, 591-628, 2004.
Maire, V., Martre, P., Kattge, J., Gastal, F., Esser, G., Fontaine, S., and Soussana, F.: The coordination of leaf photosynthesis links C and N fluxes in C_3 plant species, PLos ONE, 7, e38245, 2012.
Maire, V., Wright, I. J., Prentice, I. C., Batjes, N. H., Bhaskar, R., van Bodegom, P. M., Cornwell, W. K., Ellsworth, D., Niinemets, Ü., Ordonez, A., Reich, P. B., and Santiago, L. S.: Global effects of soil and climate on leaf photosynthetic traits and rates, Global Ecology and Biogeography, 24, 706-717, 2015.
Makino, A. and Osmond, B.: Effects of nitrogen nutrition on nitrogen partitioning between chloroplasts and mitochondria in pea and wheat, Plant ~~Physiol~~Physiology, 96, 355-362, 1991.
Manter, D. K. and Kerrigan, J.: A/C_i curve analysis across a range of woody plant speices: influence of regression analysis parameters and mesophyll conductance, Journal of Experimental Botany, 55, 2581-2588, 2004.

Maroco, J. P., Breia, E., Faria, T., Pereira, J. S., and Chaves, M. M.: Effects of long-term exposure to elevated CO_2 and N fertilization on the development of photosynthetic capacity and biomass accumulation in *Quercus suber* L. , Plant, Cell & Environment, 25, 105-113, 2002.

Martin, B., Martensson, O., and Öquist, G.: Seasonal effects on photosynthetic electron transport and fluorescence properties in isolated chloroplasts of *Pinus sylvestris*, Physiologia Plantarum, 44, 102-109, 1978.

Mayer, D. G. and Butler, D. G.: Statistical validation, Ecological Modelling, 68, 21-32, 1993.

McDowell, N.: Mechanisms linking drought, hydraulics, carbon metabolism, and vegetation mortality, Plant Physiology, 155, 1051-1059 2011.

McMurtrie, R. E., Iversen, C. M., Dewar, R. C., Medlyn, B. E., Näsholm, T., Pepper, D. A., and Norby, R. J.: Plant root distributions and nitrogen uptake predicted by a hypothesis of optimal root foraging, Ecology and Evolution, 2, 1235-1250, 2012.

Medlyn, B. E., Badeck, F.-W., De Pury, D. G. G., Barton, C. V. M., Broadmeadow, M., Ceulemans, R., De Angelis, P., Forstreuter, M., Jach, M. E., Kellomäki, S., Laitat, E., Marek, M., Philippot, S., Rey, A., Strassemeyer, J., Laitinen, K., Liozon, R., Portier, B., Proberntz, P., Wang, K., and Jarvis, P. G.: Effects of elevated $[CO_2]$ on photosynthesis in European forest species: a meta-analysis of model parameters, Plant, Cell & Environment, 22, 1475-1495, 1999.

Medlyn, B. E., Dreyer, E., Ellsworth, D., Forstreuter, M., Harley, P. C., Kirschbaum, M. U. F., Le Roux, X., Montpied, P., Strassemeyer, J., Walcroft, A., Wang, K., and Loustau, D.: Temperature response of parameters of a biochemically based model of photosynthesis. II. A review of experimental data, Plant Cell Environment, 25, 1167-1179, 2002a.

Medlyn, B. E., Duursma, R. A., Eamus, D., Ellsworth, D. A., Prentice, I. C., Barton, C. V. M., Crous, K. Y., De Angelis, P., Freeman, M., and Wingate, L.: Reconciling the optimal and empirical approaches to modelling stomatal conductance, Global Change Biology, 10, 1365-2486, 2011.

Medlyn, B. E., Loustau, D., and Delzon, S.: Temperature response of parameters of a biochemically based model of photosynthesis. I. Seasonal changes in mature maritime pine (*Pinus pinaster* Ait.), Plant, Cell & Environment, 25, 1155-1165, 2002b.

Medlyn, B. E., Robinson, B. A., Clement, R., and McMurtrie, R. E.: On the validation of models of forest CO_2 exchange using eddy covariance data: some perils and pitfalls, Tree Physiology, 25, 839-857, 2005.

Meehl, G. A., Boer, G. J., Covey, C., Latif, M., and Stouffer, R. J.: The Coupled Model Intercomparison Project (CMIP), Bulletin of the American Meteorological Society, 81, 313-318, 2000.

Miao, Z., Xu, M., Lathrop, R. G., and Wang, Y.: Comparison of the A–Cc curve fitting methods in determining maximum ribulose 1·5-bisphosphate carboxylase/oxygenase carboxylation rate, potential light saturated electron transport rate and leaf dark respiration, Plant, Cell & Environment, 32, 109-122, 2009.

Moorcroft, P. R., Hurtt, G. C., and Pacala, S. W.: A method for scaling vegetation dynamics: the ecosystem demography model (ED), ~~Ecol Monogr~~Ecological Monographs, 71, 557-586, 2001.

Moran, E. V., Hartig, F., and Bell, D. M.: Intraspecific trait variation across scales: implications for understanding global change responses, Global Change Biology, doi: 10.1111/gcb.13000, 2015. n/a-n/a, 2015.

Niinemets, Ü. and Tenhunen, J. D.: A model separating leaf structural and biphysiological effects on carbon gain along light gradients for the shade-tolerant species *Acer saccharum*, Plant, Cell & Environment, 20, 845-866, 1997.

Oleson, K. W., Lawrence, D. M., Bonan, G. B., Drewniak, B., Huang, M., Koven, C. D., Levis, S., Li, F., Riley, W. J., Subin, Z. M., Swenson, S. C., Thornton, P. E., Bozbiyik, A., Fisher, R., Kluzek, E., Lamarque, J.-F., Lawrence, P. J., Leung, L. R., Lipscomb, W., Muszala, S., Ricciuto, D. M., Sacks, W., Sun, Y., Tang, J., and Yang, Z.-L.: Technical Description of version 4.5 of the Community Land Model (CLM). NCAR Technical Note NCAR/TN-503+STR, National Center for Atmospheric Research, Boulder, CO, 2013.

Öquist, G., Brunes, L., Hällgren, J.-E., Gezelius, K., Hallén, M., and Malmberg, G.: Effects of artificial frost hardening and winter stress on net photosynthesis, photosynthetic electron transport and RuBP carboxylase activity in seedlings of *Pinus sylvestris*, Physiologia Plantarum, 48, 526-531, 1980.
Prentice, I. C., Dong, N., Gleason, S. M., Maire, V., and Wright, I. J.: Balancing the costs of carbon gain and water transport: testing a new theoretical framework for plant functional ecology, Ecology Letters, 17, 82-91, 2014.
Raddatz, T., Reick, C., Knorr, W., Kattge, J., Roeckner, E., Schnur, R., Schnitzler, K. G., Wetzel, R. G., and Jungclaus, J.: Will the tropical land biosphere dominate the climate-carbon cycle feedback during the twenty-first century?, Climate Dynamics, 29, 565-574, 2007.
Reich, P. B., Kloeppel, B. D., Ellsworth, D., and Walters, M. B.: Different photosynthesis nitorgen relations in decidious hardwood and evergreen coniferous tree species Oecologia, 104, 24-30, 1995.
Reich, P. B. and Oleksyn, J.: Global patterns of plant leaf N and P in relation to temperature and latitude, PNAS, 101, 11001-11006, 2004.
Reich, P. B., Walters, M. B., Tjoelker, M. G., Vanderklein, D., and Buschena, C.: Photosynthesis and respiration rates depend on leaf and root morphology and nitrogen concentration in nine boreal tree species differing in relative growth rate, Functional Ecology, 12, 395-405, 1998.
Riebeek, H.: The Carbon Cycle, NASA Earth Observatory, http://earthobservatory.nasa.gov/Features/CarbonCycle/, 2011.
Ripullone, F., Grassi, G., Lauteri, M., and Borghetti, M.: Photosynthesis-nitrogen relationships: interpretation of different patterns between *Pseudotsuga menziesii* and *Populus* x *euroamericana* in a mini-stand experiment, Tree Physiology, 23, 137-144, 2003.
Rogers, A.: The use and misuse of $V_{c,max}$ in earth system models, Photosynthesis Research, 119, 1-15, 2014.
Ryan, M. G.: Foliar maintenance respiration of subalpine and boral trees and shrubs in relation to nitrogen concentration, Plant, Cell & Environment, 18, 765-772, 1995.
Schaefer, K., Schwalm, C. R., Williams, C., Arain, M. A., Barr, A., Chen, J. M., Davis, K. J., Dimitrov, D., Hilton, T. W., Hollinger, D. Y., Humphreys, E., Poulter, B., Raczka, B. M., Richardson, A. D., Sahoo, A., Thornton, P., Vargas, R., Verbeeck, H., Anderson, R., Baker, I., Black, T. A., Bolstad, P., Chen, J., Curtis, P. S., Desai, A. R., Dietze, M., Dragoni, D., Gough, C., Grant, R. F., Gu, L., Jain, A., Kucharik, C., Law, B., Liu, S., Lokipitiya, E., Margolis, H. A., Matamala, R., McCaughey, J. H., Monson, R., Munger, J. W., Oechel, W., Peng, C., Price, D. T., Ricciuto, D., Riley, W. J., Roulet, N., Tian, H., Tonitto, C., Torn, M., Weng, E., and Zhou, X.: A model-data comparison of gross primary productivity: Results from the North American Carbon Program site synthesis, Journal of Geophysical Research: Biogeosciences, 117, G03010, 2012.
Schymanski, S. J., Sivapalan, M., Roderick, M. L., Hutley, L. B., and Beringer, J.: An optimality-based model of the dynamic feedbacks between natural vegetation and the water balance, Water Resources Research, 45, W01412, 2009.
Sellers, P. J., Dickinson, R., Randall, D. A., Betts, A. K., Hall, F. G., Berry, J. A., Collatz, G. J., Denning, A. S., Mooney, H. A., Nobre, A. D., Sato, N., Field, C. B., and HendersonSellers, A.: Modeling the exchanges of energy, water, and carbon between continents and the atmosphere, Science, 275, 502-509, 1997.
Sitch, S., Smith, B., Prentice, I. C., Arneth, A., Bondeau, A., Cramer, W., Kaplan, J. O., Levis, S., Lucht, W., Sykes, M. T., Thonicke, K., and Venevsky, S.: Evaluation of ecosystem dynamics, plant geography and terrestrail carbon cycling in the LPJ dynamic global vegetation model, Global Change Biology, 9, 161-185, 2003.
Smith, B., Prentice, I. C., and Sykes, M. T.: Representation of vegetation dynamics in the modelling of terrestrial ecosystems: comparing two contrasting approaches within European climate space, Global Ecology and Biogeography, 10, 621-637, 2001.
Smith, E.: The influence of light and carbon dioxide on photosynthesis, General Physiology, 20, 807-830, 1937.

Song, Y. H., Ito, S., and Imaizumi, T.: Flowering time regulation: photoperiod- and temperature-sensing in leaves, Trends in Plant Science, 18, 575-583, 2013.
Spreitzer, R. J. and Salvucci, M. E.: Rubisco: structure, regulatory interactions, and possibilities for a better enzyme, Annual Review of Plant Biology, 53, 449-475, 2002.
Strand, M. and Öquist, G.: Effects of frost hardening, dehardening and freezing trees on in vivo fluorescence of seedlings of Scots pine (*Pinus sylvestris* L.), Plant, Cell & Environment, 11, 231-238, 1988.
Taylor, K. E., Stouffer, R. J., and Meehl, G. A.: An overview of CMIP5 and the experiment design, Bulletin of the American Meteorological Society, 93, 485-498, 2013.
Thomas, R. Q. and Williams, M.: A model using marginal efficiency of investment to analyze carbon and nitrogen interactions in terrestrial ecosystems (ACONITE Version 1), Geosci. Model Dev., 7, 2015-2037, 2014.
Valladares, F., Wright, S. J., Lasso, E., Kitajima, K., and Pearcy, R. W.: PLASTIC PHENOTYPIC RESPONSE TO LIGHT OF 16 CONGENERIC SHRUBS FROM A PANAMANIAN RAINFOREST, Ecology, 81, 1925-1936, 2000.
Van Oijen, M., Schapendonk, A., and Hoglind, M.: On the relative magnitudes of photosynthesis, respiration, growth and carbon storage in vegetation, Ann Bot-London, 105, 793-797, 2010.
Verheijen, L. M., Aerts, R., Brovkin, V., Cavender-Bares, J., Cornelissen, J. H. C., Kattge, J., and van Bodegom, P. M.: Inclusion of ecologically based trait variation in plant functional types reduces the projected land carbon sink in an earth system model, Global Change Biology, 21, 3074-3086, 2015.
Verheijen, L. M., Brovkin, V., Aerts, R., Bönisch, G., Cornelissen, J. H. C., Kattge, J., Reich, P. B., Wright, I. J., and van Bodegom, P. M.: Impacts of trait variation through observed trait–climate relationships on performance of an Earth system model: a conceptual analysis, Biogeosciences, 10, 5497-5515, 2013.
Walker, A. P., Beckerman, A. P., Gu, L., Kattge, J., Cernusak, L. A., Domingues, T. F., Scales, J. C., Wohlfahrt, G., Wullschleger, S. D., and Woodward, F. I.: The relationship of leaf photosynthetic traits – Vcmax and Jmax – to leaf nitrogen, leaf phosphorus, and specific leaf area: a meta-analysis and modeling study, Ecology and Evolution, 4, 3218-3235, 2014.
Wang, Y. P., Law, R. M., and Pak, B.: A global model of carbon, nitrogen and phosphorus cycles for the terrestrial biosphere, Biogeosciences, 7, 2261-2282, 2010.
White, M. A., Thornton, P. E., Running, S. W., and Nemani, R. R.: Parameterization and sensitivity analysis of the BIOME-BCG terrestrial ecosystem model: net primary production controls, Earth Interactions, 4, 1-85, 2000.
Whitley, R. J., Catriona, M. O., Macinnis-Ng, C., Hutley, L. B., Beringer, J., Zeppel, M., Williams, M., Taylor, D., and Eamus, D.: Is productivity of mesic savannas light limited or water limited? Results of a simulation study, Global Change Biology, 17, 3130-3149, 2011.
Wieder, W. R., Cleveland, C. C., Lawrence, D. M., and Bonan, G. B.: Effects of model structural uncertainty on carbon cycle projections: biological nitrogen fixation as a case study Environmental Research Letters, 10, 044016, 2015.
Wilson, K. B., Baldocchi, D. D., and Hanson, P. J.: Leaf age affects the seasonal pattern of photosynthetic capacity and net ecosystem exchange of carbon in a deciduous forest, Plant, Cell & Environment, 24, 571-583, 2001.
Wright, I. J., Reich, P. B., Westoby, M., Ackerly, D. D., Baruch, Z., Bongers, F., Cavender-Bares, J., Chapin, T., Cornelissen, J. H. C., Diemer, M., Flexas, J., Garnier, E., Groom, P. K., Gulias, J., Hikosaka, K., Lamont, B. B., Lee, T. D., Lee, W., Lusk, C. H., Midgley, J. J., Navas, M.-L., Niinemets, Ü., Olesksyn, J., Osada, N., Poorter, H., Poot, P., Prior, L., Pyankov, V. I., Roumet, C., Thomas, S. C., Tjoelker, M. G., Veneklaas, E. J., and Villar, R.: The worldwide leaf economics spectrum, Nature, 428, 821-827, 2004.
Wullschleger, S. D.: Biochemical limitations to carbon assimilation in C_3 plants: a retrospective analysis of A/C_i curves from 109 species, Journal of Experimental Botany 44, 907-920, 1993.
Xu, C., Fisher, R., Wullschleger, S. D., Wilson, C. J., Cai, M., and McDowell, N.: Toward a mechanistic modeling of nitrogen limitation on vegetation dynamics, PLos ONE, 7, e37914, 2012.

Xu, L. and Baldocchi, D. D.: Seasonal trends in photosynthetic parameters and stomatal conductance of blue oak (*Quercus douglasii*) under prolonged summer drought and high temperature, Tree Physiology, 23, 865-877, 2003.
Yamori, W., Suzuki, K., Noguchi, K. O., Nakai, M., and Terashima, I.: Effects of Rubisco kinetics and Rubisco activation state on the temperature dependence of the photosynthetic rate in spinach leaves from contrasting growth temperatures, Plant, Cell & Environment, 29, 1659-1670, 2006.

9. Tables

Table 1 Mean values of parameters obtained by using the Differential Evolution Adaptive Metropolis Snooker updater (DREAM-ZS) sampling technique when TRF1 and TRF2 were used. TRF1 was a temperature response function that considered the potential for acclimation to growth temperature while TRF2 was a temperature response function that did not consider change in temperature response coefficients to growth temperature. The parameters include; J_{maxb0} (unitless) - baseline proportion of nitrogen allocated for electron transport rate, J_{maxb1} (unitless) - electron transport rate response to light availability, $t_{c,j0}$ (unitless) – baseline ratio of Rubisco limited rate to light limited rate, and H (unitless) - electron transport rate response to relative humidity. The standard deviations are shown in the parentheses.

Statistics	J_{maxb0}	J_{maxb1}	$t_{c,j0}$	H
TRF1	0.0311 (0.0004)	0.1745 (0.0002)	0.8054 (0.0015)	6.0999 (0.2416)
TRF2	0.0322 (0.0002)	0.1695 (0.0006)	0.7760 (0.0031)	5.7139 (0.0354)

10. Figures

Figure captions

Figure 1 Percentage of variations (r^2, ME; model efficiency) in observed $V_{c,max25}$ (μmol CO_2 m^{-2} s^{-1}) explained by modeled $V_{c,max25}$ (a, c) and in observed J_{max25} (μmol electron m^{-2} s^{-1}) explained by modeled J_{max25} (b, d) across all of the species, using TRF1 (a, b) and TRF2 (c, d), where the nitrogen allocation model, the environmental variables, leaf mass per leaf area, and the leaf nitrogen contents were used. TRF1 was a temperature response function that considered the potential for acclimation to growth temperature while TRF2 was a temperature response function that did not consider change in temperature response coefficients to growth temperature. The r^2 is derived by a linear regression between observed and modeled values. The dashed line is the 1:1 line.

Figure 2 Effects of changes in nitrogen allocation parameters on the predicted $V_{c,max25}$ (μmol CO_2 m^{-2} s^{-1}) (a, c) and J_{max25} (μmol electron m^{-2} s^{-1}) (b, d). Each parameter (J_{maxb0}, J_{maxb1}, $t_{c,j0}$, and H) was varied one at a time by +/-15% of its value by using either TRF1 (a, b) or TRF2 (c, d). TRF1 was a temperature response function that considered the potential for acclimation to growth temperature while TRF2 was a temperature response function that did not consider change in temperature response coefficients to growth temperature. The environmental variables (day length; 14 hours, daytime radiation; 182 W m^{-2}, temperature; 14^{o}C, relative humidity; 0.6 (unitless), and carbon dioxide; 393 ppm) were held fixed. Firstly, $V_{c,max25}$ and J_{max25} values were obtained at changed parameter value. Next, percentage changes in $V_{c,max25}$ and J_{max25} were calculated relative to the baseline values of $V_{c,max25}$ and J_{max25}.

1175 **Figure 3** Effects of environmental variables (day length, daytime radiation, temperature, relative
1176 humidity, and carbon dioxide) on predicted $V_{c,max25}$ (μmol CO_2 m^{-2} s^{-1}) (a, c) and J_{max25} (μmol
1177 electron m^{-2} s^{-1}) (b, d). Each environmental variable (day length; 14 hours, daytime radiation;
1178 182 W m^{-2}, temperature; 14^{o}C, relative humidity; 0.6 (unitless), and carbon dioxide; 393 ppm)
1179 was varied one at a time by +/-15%. TRF1 (a, b) and TRF2 (c, d) were used, with the parameters
1180 (J_{maxb0}, J_{maxb1}, $t_{c,j0}$, and H) being held fixed. TRF1 was a temperature response function that
1181 considered the potential for acclimation to growth temperature while TRF2 was a temperature
1182 response function that did not consider change in temperature response coefficients to growth
1183 temperature. Firstly, $V_{c,max25}$ and J_{max25} values were obtained at changed environmental
1184 condition. Next, percentage changes in $V_{c,max25}$ and J_{max25} were calculated relative to the baseline
1185 values of $V_{c,max25}$ and J_{max25}.
1186
1187 **Figure 4** Summer season photosynthetic capacity for the top leaf layer in the canopy ($V_{c,max25}$;
1188 μmol CO_2 m^{-2} s^{-1} (a), J_{max25}; μmol electron m^{-2} s^{-1} (c)) under historical climatic conditions and the
1189 difference in either $V_{c,max25}$ (b) or J_{max25} (d) due to changed climatic conditions. Difference in the
1190 photosynthetic capacity was calculated as that under future climate minus that under historical
1191 climate. Ten-year monthly averages of climatic conditions for the past (1995 – 2004) and the
1192 future (2090-2099) were used to drive the model. The model was run by using TRF1, which was
1193 a temperature response function that considered the potential for acclimation to growth
1194 temperature.
1195
1196 **Figure 5** Sensitivity of $V_{c,max25}$ (μmol CO_2 m^{-2} s^{-1}) to changes in environmental variables (a;
1197 Temperature, b; Radiation, c; Humidity, and d; CO_2) at the global scale by using TRF1. TRF1

was a temperature response function that considered the potential for acclimation to growth temperature. The ~~changes in~~sensitivity analysis is conducted by changing the value of individual environmental ~~conditions are based on~~variable using 10-year monthly averages of climatic conditions for the past (1995-2004) ~~and~~versus the future (2090-2099~~).~~) for each individual grid across the globe.

Figure 6 Sensitivity of J_{max25} (μmol electron m^{-2} s^{-1}) to changes in environmental variables (a; Temperature, b; Radiation, c; Humidity, and d; CO_2) at the global scale using TRF1. TRF1 was a temperature response function that considered the potential for acclimation to growth temperature. The ~~changes in~~sensitivity analysis is conducted by changing the value of individual environmental ~~conditions are based on~~variable using 10-year monthly averages of climatic conditions for the past (1995~~-~~-2004) ~~and~~versus the future (2090-2099~~).~~) for each individual grid across the globe.

Figure 7 Percentage differences in A_{net} (μmol CO_2 m^{-2} s^{-1}) for using $V_{c,max25}$ (μmol CO_2 m^{-2} s^{-1}) and J_{max25} (μmol electron m^{-2} s^{-1}) based on historical climate and that using $V_{c,max25}$ and J_{max25} based on future climate conditions. TRF1 (a) and TRF2 (b) were used in the model simulations. TRF1 was a temperature response function that considered the potential for acclimation to growth temperature while TRF2 was a temperature response function that did not consider change in temperature response coefficients to growth temperature. 10-year monthly averages of climatic conditions for the past (1995 – 2004) and the future (2090-2099) were used to drive the model.

1221

1222 **Figures**

1223 Fig. 1

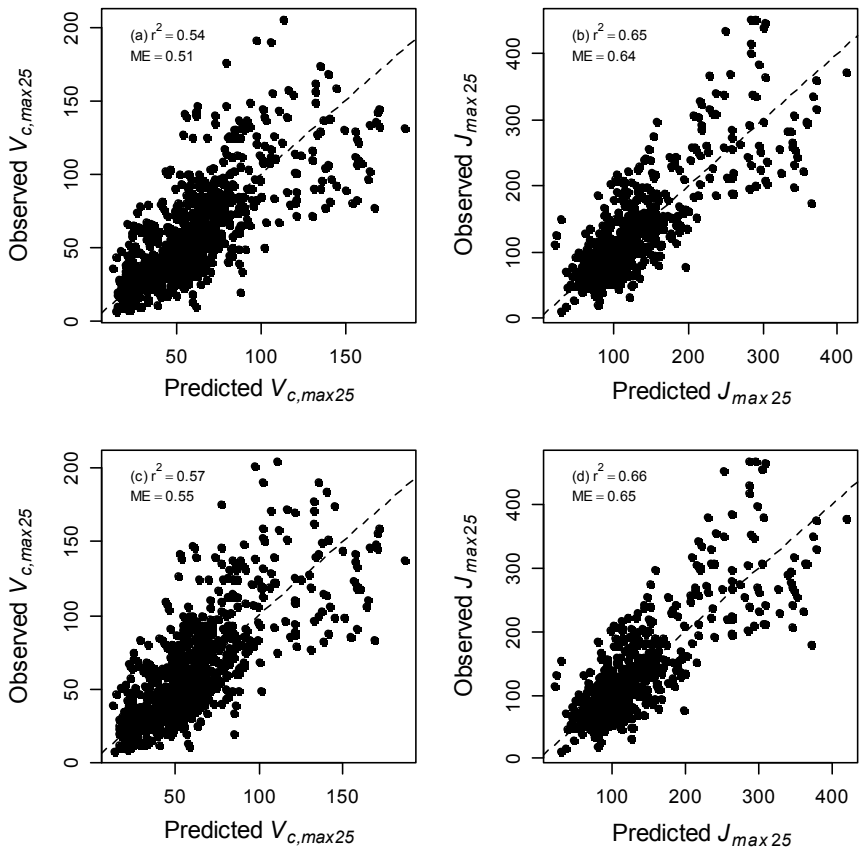

1224

1225

1226 Fig. 2

1227

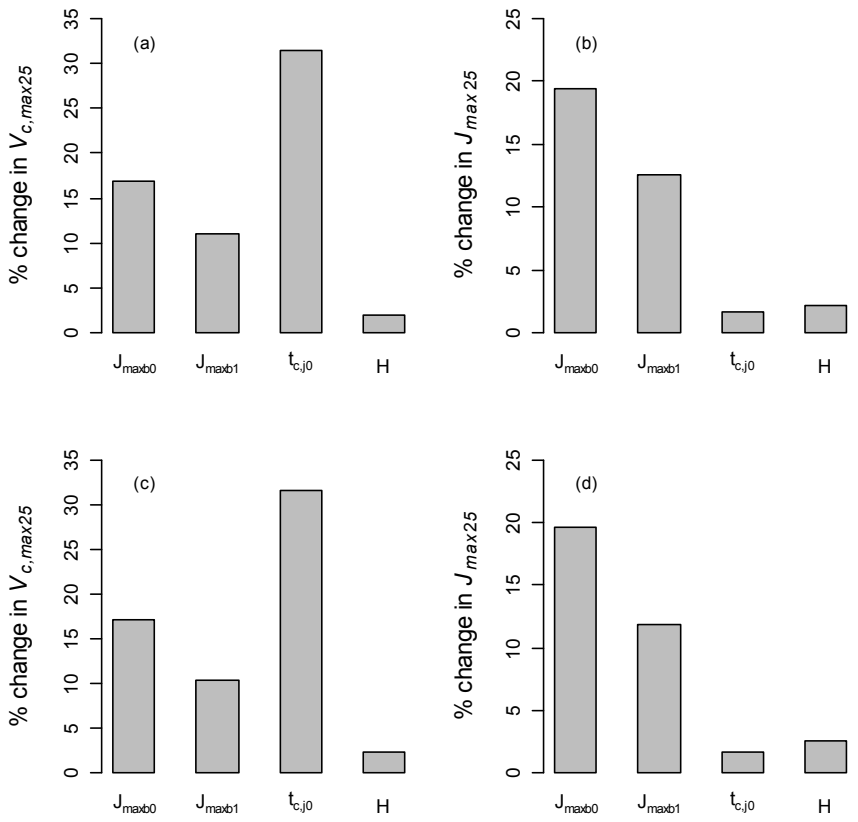

1228

1229

1230 Fig. 3

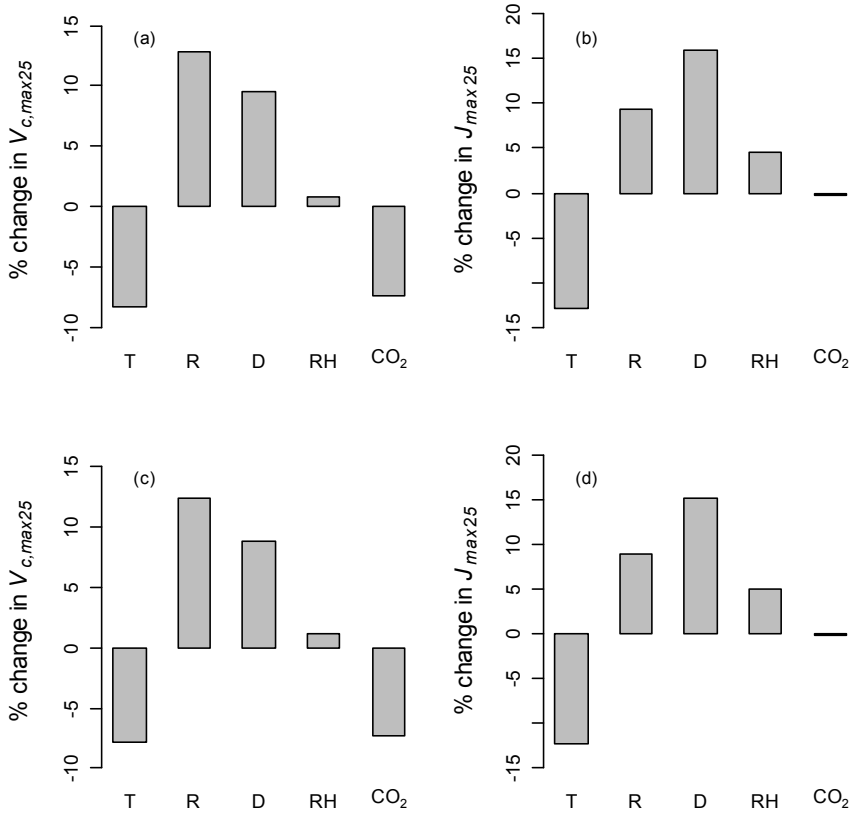

1231

1232

1233 Fig. 4

1234

1235

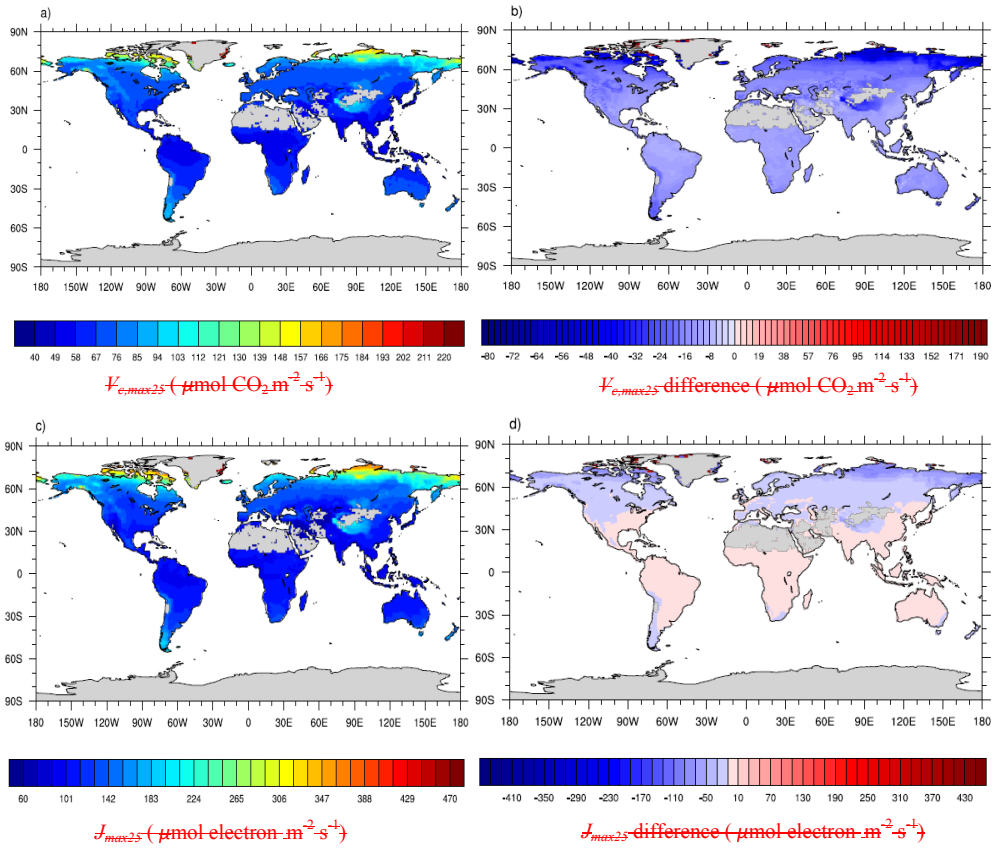

1236 ~~$V_{c,max25}$ (μmol CO_2 m^{-2} s^{-1})~~ ~~$V_{c,max25}$ difference (μmol CO_2 m^{-2} s^{-1})~~

1237 ~~J_{max25} (μmol electron m^{-2} s^{-1})~~ ~~J_{max25} difference (μmol electron m^{-2} s^{-1})~~

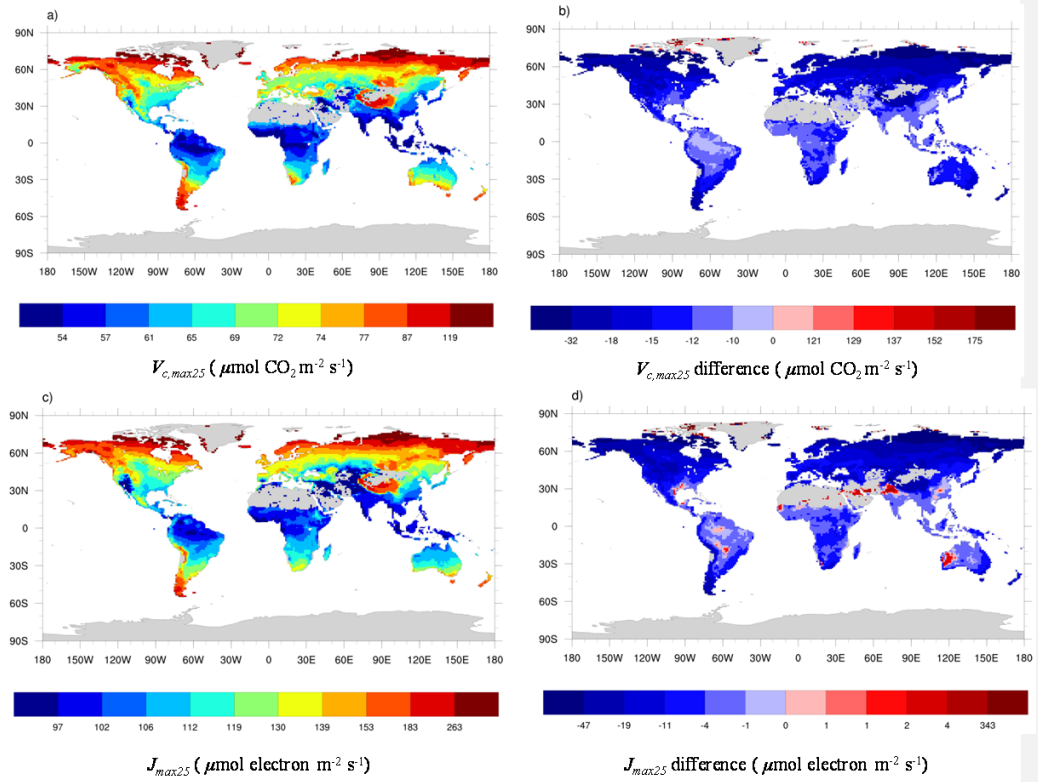

$V_{c,max25}$ (μmol CO_2 m^{-2} s^{-1})

$V_{c,max25}$ difference (μmol CO_2 m^{-2} s^{-1})

J_{max25} (μmol electron m^{-2} s^{-1})

J_{max25} difference (μmol electron m^{-2} s^{-1})

1242 Fig. 5

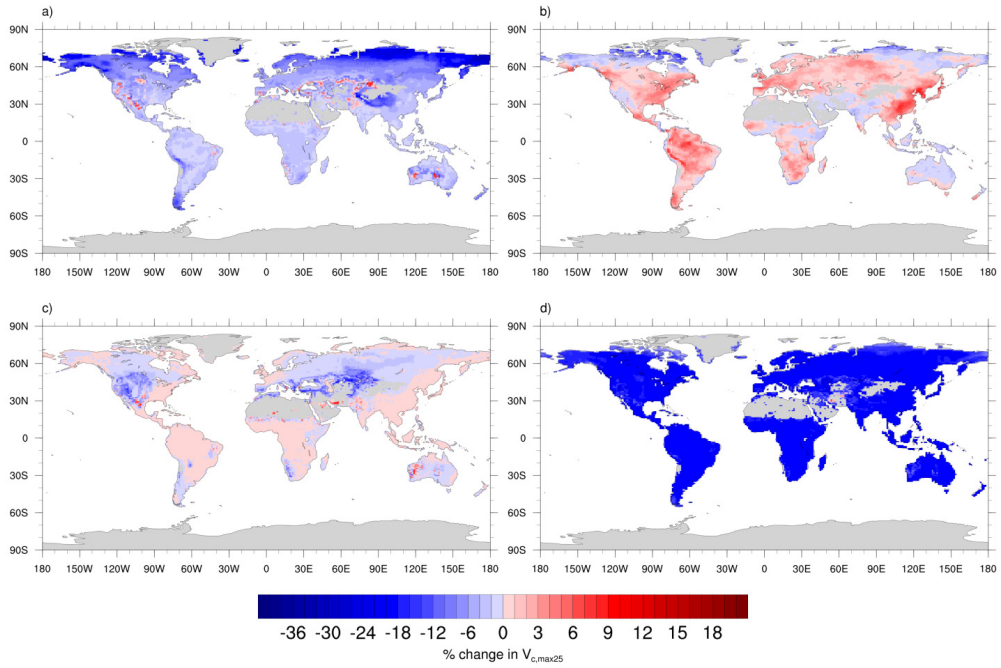

1243

1244

1245

1246 Fig. 6

1247

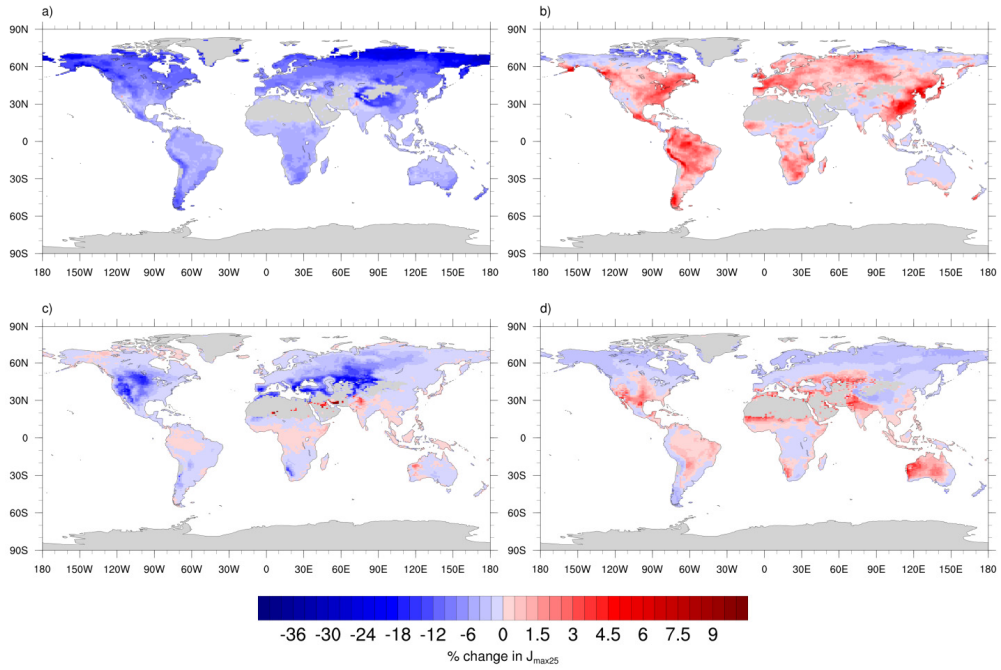

1248

1249

Fig. 7

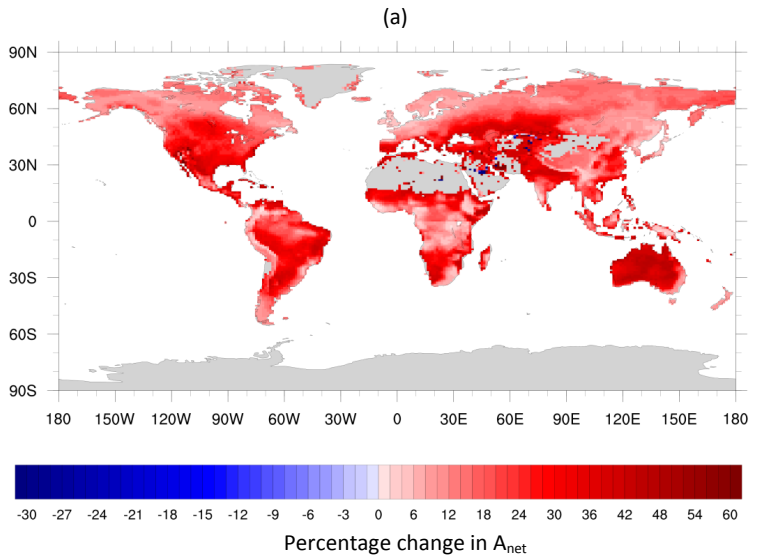
(a)
90N
60N
30N
0
30S
60S
90S
180 150W 120W 90W 60W 30W 0 30E 60E 90E 120E 150E 180
-30 -27 -24 -21 -18 -15 -12 -9 -6 -3 0 6 12 18 24 30 36 42 48 54 60
Percentage change in A_{net}
(b)
90N
60N
30N
0
30S
60S
90S
180 150W 120W 90W 60W 30W 0 30E 60E 90E 120E 150E 180
-30 -27 -24 -21 -18 -15 -12 -9 -6 -3 0 6 12 18 24 30 36 42 48 54 60
Percentage change in A_{net}